AD-A015 131

IMPACT RESPONSE CHARACTERISTICS OF POLYMERIC MATRICES

William B. Hillig

General Electric Corporate Research and Development

Prepared for:

Naval Air Systems Command

August 1975

DISTRIBUTED BY:

NTIS

National Technical Information Service
U. S. DEPARTMENT OF COMMERCE

279181

ADA015131

IMPACT RESPONSE CHARACTERISTICS OF POLYMERIC MATRICES

FINAL REPORT

(12 February 1974 to 11 May 1975)

AUGUST 1975

By

W. B. Hillig

Prepared Under Contract N00019-74-C-0147

for

Naval Air Systems Command
Department of the Navy
Washington, D. C. 20361

DDC
RECEIVED
SEP 25 1975
C

By

Corporate Research and Development
General Electric Company
Schenectady, New York

APPROVED FOR PUBLIC RELEASE; DISTRIBUTION UNLIMITED

Reproduced by
NATIONAL TECHNICAL
INFORMATION SERVICE
U.S. Department of Commerce
Springfield, VA 22151

SRD-75-083

Unclassified
Security Classification

DOCUMENT CONTROL DATA · R & D

(Security classification of title, body of abstract and indexing annotation must be entered when the overall report is classified)

1 ORIGINATING ACTIVITY (Corporate author) General Electric Company, Corporate Research and Development, PO Box 8, Schenectady, NY 12301	2a. REPORT SECURITY CLASSIFICATION Unclassified 2b. GROUP

3 REPORT TITLE

Impact Response Characteristics of Polymeric Matrices

4 DESCRIPTIVE NOTES (Type of report and inclusive dates)

Final Report - 12 February 1974 to 11 May 1975

5. AUTHOR(S) (First name, middle initial, last name)

William B. Hillig

6 REPORT DATE August 1975	7a. TOTAL NO. OF PAGES 86	7b. NO. OF REFS 7
8a. CONTRACT OR GRANT NO. N00019-74-C-0147 b. PROJECT NO. c. d.	9a. ORIGINATOR'S REPORT NUMBER(S) SRD-75-083 9b. OTHER REPORT NO(S) (Any other numbers that may be assigned this report)	

10. DISTRIBUTION STATEMENT

APPROVED FOR PUBLIC RELEASE; DISTRIBUTION UNLIMITED

11. SUPPLEMENTARY NOTES	12. SPONSORING MILITARY ACTIVITY Naval Air Systems Command Department of the Navy Washington, DC

13. ABSTRACT

Impact/indentation velocity measurements on polycarbonate (PC) and polymethylmethacrylate (PMMA) have been measured to 6000 inches/minute using a 4.5 mm diameter ball as the impacting object. The "best" force versus penetration depth values are given covering the range .0002 inches/minute to the maximum. Load relaxation measurements are reported and are found to have a characteristic time-decay constant inversely proportional to the impact velocity. This anomalous result causes a sensitive time dependence to be obscured under ordinary conditions. The deformation zone is found to consist of densified material and appears to result from an anelastic yielding. Models, analyses, and interpretations of the results are developed. The phenomena are believed to be fairly broadly applicable to other polymers.

1473

Unclassified
Security Classification

14 KEY WORDS	LINK A		LINK B		LINK C	
	ROLE	WT	ROLE	WT	ROLE	WT
Impact damage of polymers Indentation Stress relaxation						

ABSTRACT

Impact/indentation velocity measurements on polycarbonate (PC) and polymethylmethacrylate (PMMA) have been measured to 6000 inches/minute using a 4.5 mm diameter ball as the impacting object. The "best" force versus penetration depth values are given covering the range .0002 inches/minute to the maximum. Load relaxation measurements are reported and are found to have a characteristic time-decay constant inversely proportional to the impact velocity. This anomalous result causes a sensitive time dependence to be obscured under ordinary conditions. The deformation zone is found to consist of densified material and appears to result from an anelastic yielding. Models, analyses, and interpretations of the results are developed. The phenomena are believed to be fairly broadly applicable to other polymers.

TABLE OF CONTENTS

Preceding page blank

SUMMARY

This report describes our recent progress at gaining an understanding of the impact response of polymethylmethacrylate (PMMA), polycarbonate (PC), and epoxy resins when struck by a small hard object. This work has concentrated on the reaction force due to the indentation of steel spheres into the resin as a function of velocity, depth, and size. In particular our aims were:

1. Extend the force-indentation measurements to the highest available (constant) velocities in order to detect, if possible, the onset of the limiting elastic behavior, and to provide a better basis for extrapolation to higher velocities.
2. Determine the relaxation behavior directly by abruptly halting the indentation process at predetermined depths, velocities, and ball sizes, and following the time delay of the force.
3. Determine the effect of change of velocity on the force-indentation behavior to see how to take this into account in a free impact, i.e., free deceleration encounter.
4. Investigate the mechanical uniformity of the test materials to see whether this can explain the occasional marked differences in the responses of replicate tests on the same materials under identical conditions.
5. Determine what deformation processes are involved and to what extent; these processes include elastic, anelastic, viscoelastic, and/or densification deformations.

The new results extend the data to 6000 inches/minute. The results show that even at these high velocities, the material still is not behaving elastically. This means that extrapolation of the response to higher velocities is uncertain.

The relaxation of the indentation force was directly observed by following the decay in force when the indentation was abruptly halted. The decay law, instead of being exponential, was found to obey $F(t) = F(o)(1+AT)^{-B}$, in which A can be identified as the inverse relaxation time. Remarkably for both PC and PMMA, A was found to be approximately proportional to the velocity at which the indentation had been performed. This means that during a normal indentation measurement at constant velocity the relaxation of the force for a given increase in penetration depth is approximately constant, independent of velocity. Thus, in spite of a very strong intrinsic time dependence of the impact response process, the direct observations at constant velocity give the illusion of being only weakly time dependent. This kind of relaxation behavior manifests itself particularly under conditions of changing velocity. Accordingly, the indentation response of PC and PMMA was determined in which the velocity was discontinuously increased and decreased one hundred fold.

Indentation was also studied as a function of ball size at two velocities. The Meyer law, $Force = Cr^n$, inwhich C is an experimental constant dependent on the ball size, material, and velocity, is often used to provide information about the deformation process. For elastic materials, $n = 3$; for strain hardening materials, $n \approx 2.5$; and for ideal plastic materials, $n = 2$. Our results show that n is not constant, suggesting that several mechanisms are operating.

Macro indentation measurements performed on PC and PMMA showed that substantial local variations in hardness occur. The uniformity of PC exceeds that of PMMA.

Finally, observations were made of the yield zone underneath the indentations. The results show that substantial densification occurs with PC, PMMA, and epoxy. Furthermore, the process appears to be characterized by a recoverable anelastic yielding. Some estimates of yield stresses were made based on the Hill elastic-plastic analysis.

IMPACT RESPONSE CHARACTERISTICS OF POLYMERIC MATRICES

1. INTRODUCTION

Damage to structural materials due to ballistic encounters with small objects is a matter of considerable practical concern. Such commonplace events are complex, are not well understood, nor are they well documented. This report describes the accomplishments during the last year as part of a long-range effort aimed at gaining an understanding of the phenomena associated with impact encounters, so as (1) to develop a useful methodology for characterizing the responses, (2) to determine which basic physical properties are the dominant ones leading to a predictive theory, and (3) to provide a rational basis for the design of better impact resistant materials. In this investigation, we are continuing to concentrate on the response of polymethylmethacrylate (PMMA), polycarbonate (PC), and epoxy resins to constant velocity encounters. Our prior work[1,2] was aimed at getting basic data of impact force as a function of time and depth of penetration, over a wide range of velocities. The present work extends this information to even greater velocities up to 6000 inches/minute for PMMA and PC. In addition much of the effort was exploratory, being concerned with establishing the nature of several basic constituent processes. This work builds on our previous efforts which are briefly summarized next.

1.1 Previous Studies

Our continuing concern has been to understand the primary response at the immediate site of the impact. This encounter produces an impulse wave which can also produce damage remote

from the site of the original impact. However, such secondary response is beyond the scope of our work. Originally our intent was to study the deceleration and impulse resulting from an encounter with a free flying projectile. However, it became apparent that great simplification could be attained by keeping the velocity fixed throughout the encounter. Even so, the response of PMMA, PC, and epoxy was complex. A standard 4.5 mm diameter steel ball bearing was used as the impacting body for most experiments. However, conical indenters having cone angles ranging from 20° to 75° were also used. The balls were impressed into the polymers over a 5 to 7 decade range of velocities, the lowest velocity being .0002 inches/minute. The force F versus penetration depth x data was given by

$$F = Kx^{3/2}\phi \ ,$$

in which K is an experimentally determined constant, and ϕ is a correction term defined so that $\lim \phi = 1$ as $x \to 0$. If the material were elastic, then $\phi = 1$, and $K = (4/3)\, E\sqrt{R}/(1-\nu^2)$, in which E is the Young's modulus, R is the ball radius, and ν is the Poisson ratio. However, the polymers are not elastic, even though they are well below their glass transition temperature. Thus, ϕ depends on x and/or time. If the polymers behaved as viscoelastic solids, as initially expected, then from a knowledge of ϕ , the relaxation modulus for the polymers could be deduced. This requires the use of LaPlace transforms and places certain restrictions, out of considerations of mathematical convenience, on the form in which ϕ can be expressed. Such a form was developed which permitted the data to be accurately represented as an empirical law. However, the resultant computed relaxation modulus was not a monontonically decreasing function of time as is physically required. From this it was concluded that these polymeric materials were not behaving like viscoelastic solids.

Other factors considered included the possibility that (1) adiabatic heating could lead to substantial departures from expected viscoelastic response, (2) large strain effects substantially alter the response expected from analyses based on infinitesimal strains, (3) some kind of nonlinear relaxation processes are occurring, and (4) that time-independent plastic flow is involved. The first item was dismissed on the basis of indentation measurements made over a range of temperatures. The second was at variance with an analysis based on large strain deformation and was judged not a major factor. The third factor cannot literally be true in the sense that ductile deformation cannot occur instantaneously. Therefore, items (3) and (4) really merge into the same category.

Since force F was measured as a function of depth over a wide range of velocities, it was possible to develop empirical "equations of state" which related F to depth x, time t, and velocity μ. In constant velocity experiments, t is always proportional to x. However, by suitable comparison at different velocities, but at constant depth or at constant time, it was possible to establish that F depended strongly on t as well as on x. Surprisingly, the time dependence at constant depth obeyed the law,

$$F(x = \text{constant}) = k \ln (t_o/t) \qquad (a)$$

where k and t_o are experimentally determined constants. Actually, time t is simply depth/velocity. This result is anomalous because it predicts that F blows up at t = 0. In contrast classical models predict:

$$F\ (x = \text{constant}) = k' \exp(-t/t_o) \quad . \qquad (b)$$

The polymers PC, PMMA, and cured epoxy have so-called glass transition temperatures that are well above the experimental temperatures. Therefore, sluggish relaxation was to be expected; and under increasingly large rates of strain, the response was expected to approach a limiting elastic law. However, over the five to seven decades range of velocities, no clear indication of such a limiting response could be found.

In summary, the force-penetration laws were determined in some considerable detail over a wide range of velocities. However, the understanding of why or how these particular response laws came about was far from complete. Certain plausible explanations were found to be not relevant, and there remained a recognition that the time-dependent behavior was not as expected. This was the state of understanding at the time the present work was undertaken.

1.2 Present Objectives

The aims of the present contract have been as follows:

1. Extend the force indentation measurements to the highest available (constant) velocities in order to detect, if possible, the onset of the limiting elastic behavior, and to provide a better basis for extrapolation to higher velocities.
2. Determine the relaxation behavior directly by abruptly halting the indentation process at predetermined depths, velocities, and ball sizes, and following the time delay of the force.
3. Determine the effect of change of velocity on the force-indentation behavior to see how to take this into account in a free impact, i.e., free deceleration encounter.
4. Investigate the mechanical uniformity of the test materials to see whether this can explain the occasional marked differences in the responses of replicate tests on the same materials under indentical conditions.

5. Determine what deformation processes are involved and to what extent; these processes include elastic, anelastic, viscoelastic, and/or densification deformations.

The experimental results and analyses relating to these objectives are presented in Sections 3 and 4.

2. MATERIALS AND SPECIMEN PREPARATION

The PC, PMMA, and epoxy materials were unchanged from those used in the previous study with the exception that the PMMA used was limited to the Rohm and Haas Plexiglas® sheet. Also, last year's study indicated that the cementing of a glass plate base to the bottom of the specimens to ensure good mating between the specimen and the base plate of the testing machine did not lead to substantial decrease in the variation between replicate runs. Hence, specimens were used as cut out of sheet stock, making sure that all burrs were removed. The standard specimen size was 1" x 1" x 0.5".

2.1 Polymethylmethacrylate

Specimens were cut from the same Type G Plexiglas® sheet PMMA (produced by Rohm and Haas) as was used in last year's study. Continuing with our former practice, the sheet was marked off in squares for cutting and a record kept so that the original location of each specimen in the sheet could be identified.

2.2 Polycarbonate

The PC resin was manufactured by the General Electric Company and is designated as Lexan® resin general purpose glazing sheet, Type 9034-112. The same sheet of 0.5" thick material was used as for last year's study. Specimens were marked and records kept as for the case of PMMA.

2.3 Epoxy

This resin was molded out of a mixture of 20% by weight of methylene dianiline with Epon® 828 resin manufactured by Shell Chemical Co. The mixture was cast into a 1/2" slab, allowed to set at room temperature to expel possible bubbles. The temperature was raised to 95°C, held for one hour, and then raised again to 145°C for two hours. Following machining to produce flat, parallel surfaces, the specimens were heated for final cure at 150°C for two additional hours.

3. EXPERIMENTAL MEASUREMENTS AND OBSERVATIONS

The reaction force on the indenter was measured under various rates of loading, indenter sizes, and times. In addition, observations were made on the materials themselves, e.g., hardness, density, and deformation geometry. In most cases, these techniques are similar to those described in detail in our previous report. Hence, only abbreviated descriptions will be given below except where substantial new features are involved.

3.1 Force as Function of Constant Velocity

3.1.1 Experimental. The indentation force versus depth data was extended to velocities up to ca. 100 inches/second using the MTS electrohydraulic mechanical test machine. In these experiments, the indenter used was the standard 4.5 mm ball. The force-time information was recorded and stored in a digital storage oscilloscope (Nicolet Model 1090) which allows a signal to be played back at any desired expansion of the time axis. This has enabled obtaining much higher time resolutions than was possible with our previous apparatus. The nature of the electrohydraulic machine is to give a crosshead displacement that is not quite as smooth a function of time as would be achieved with a screw-drive machine. As a result, even with the increased time resolution, there is some unavoidable uncertainty in the force-distance data.

In order to get some overlap between the data from the Instron machine and the MTS machine, measurements were made over the range 0.1-100 inches/minute in decade steps on PC and PMMA specimens. Measurements were generally made in triplicate. The indentation force in pounds as a function of depth and velocity is given for PC and PMMA, respectively, in Tables 3.1.1A and B.

3.1.2 Discussion of Results. The previous data on PC and PMMA augmented by the present data on the indentation behavior have been analyzed to give the "best" overall response values. This was done by plotting the force corresponding to a given

TABLE 3.1.1A

OBSERVED INDENTATION LOADS FOR PC AT VARIOUS FIXED DEPTHS

Sample Number	Velocity in/sec	$K_o \times 10^{-3}$	Load at Indicated Depth in mils								
			5	10	15	20	30	40	50	60	70
6E	0.1	91	40	100	170	235	365	495	620	730	831
6F	"	90	35	100	160	235	370	490	605	715	815
6P	"	100	35	100	170	235	365	495	610	720	829
Average		94	37	100	167	235	367	493	612	722	825
9D	1	115	46	112	188	264	408	563	702	828	956
9F	"	100	38	98	160	230	352	482	612	732	845
9L	"	110	37	102	177	252	392	527	666	798	912
Average		108	40	104	175	249	384	524	660	786	904
6I	10	119	45	120	198	283	433	583	709	843	
7P	"	114	48	120	203	280	438	578	698	810	
9J	"	137	50	126	210	306	448	606	724	836	
Average		123	48	122	204	290	440	589	710	830	
4T	100	239	75	150	250	330	500	670	820	960	
5I	"	255	75	165	240	340	510	640	810	930	
9Q	"	272	70	160	250	345	520	690	850	1000	
9V	"	165	75	140	230	310	510	680	810	940	
Average		233	74	154	243	331	510	670	823	963	

TABLE 3.1.1B

OBSERVED INDENTATION LOADS FOR PMMA AT VARIOUS FIXED DEPTHS

Sample Number	Velocity in/sec	$K_o \times 10^{-3}$	Load at Indicated Depth in mils								
			5	10	15	20	30	40	50	60	70
7B	0.1	248	70	190	300	440	710	945	1160	1365	1535
7K	"	194	70	180	310	455	715	940	1140	1308	1450
8L	"	215	80	180	305	438	698	925	1110	1280	1410
Average		219	73	183	305	444	708	937	1137	1318	1465
7M	1	252 367	60	190	338	505	810	1075	1330		
8N	"	301	100	220	360	540	870	1165	1430	1630	
8Ø	"	343	105	240	400	550	860	1120	1340	1570	1775
Average		316	88	217	366	532	847	1120	1367	(1600)	(1775)
9E	10	317	115	315	485	675	1005	1372	1750		
9M	"	360	125	355	550	750	1120	1490	1880*		
12E	"	434	130	350	530	710	1060	1440	1810*		
Average		370	123	337	522	712	1062	1436	1813		
7A	100	451	170	370	595	845	1280	1610	1910		
8I	"	414	165	350	575	820	1230	1690	1900		
8K	"	529	190	395	620	870	1315	1650	1945		
Average		465	178	372	597	845	1275	1650	1918		

*Extrapolated

penetration depth versus the log of the impact velocity over the entire range using all of the individual data points. The best curve was drawn through the data, and the values at each velocity were picked off of the curve. The procedure was performed at 5, 10, 20, 30, 40, and 50 mils. These results represent, in our judgment, the best self-consistent values covering this regime, and are given in Tables 3.1.2A and B, as well as in Figs. 3.1.2A and B. Because we have been particularly interested in the deviation of the impact behavior from the expectations based on the Hertz law, the data are also given in Figs. 3.1.2C and D in the form of $F/x^{3/2}$. As discussed in Section 1.1, this is equal to $K\phi$ and would be a constant for an ideal elastic material. The information is also presented directly as plots of F versus x in Fig. 3.1.2E and F.

The results show that a very pronounced "hardening" in the response of both PC and PMMA occurs at the higher velocities. At some point, $F/x^{3/2}$ should saturate, corresponding to elastic behavior. The observed hardening is actually more pronounced at small indentation depths. This is somewhat unexpected, since the strain is least at small indentation depths, where Hertz-like behavior is already observed. This may be a reflection of the effect of adiabatic heating, or this may indicate a more complicated viscoelastic-plastic response. If the "instantaneous" values for the Young's modulus of PC and PMMA were known, then the limiting value of $K\phi$ could be computed. The best indications are those derived from high frequency acoustic measurements which give the values[3] 404 ksi at 1 MHz and 843 ksi at 3 MHz for PC and PMMA, respectively. The corresponding estimates for the limiting value of $K\phi$ are 180 and 370 ksi/inch$^{3/2}$. Comparison with Figs. 3.1.2C and D shows that these values have already been exceeded. Another estimate[4] for the limiting modulus results from extrapolating the values derived from measurements as a function of temperature at 10 KHz to 0°K. For PMMA this gives a value of 1300 ksi, corresponding to 570 ksi/inch$^{3/2}$ for $K\phi$. (Such an estimate is not

TABLE 3.1.2A

BEST AVERAGED VALUES OF FORCE VS INDENTATION DEPTH BEHAVIOR OF PC AS A FUNCTION OF INDENTATION VELOCITY USING 4.5 mm DIAMETER STEEL INDENTER

Velocity	Load in Pounds at Indicated Depth in Mils					
in/min	5	10	20	30	40	50
.0002	40	99	219			
.002	40	100	220	340	460	558
.02	40	101	222	342	462	560
.2	40	102	225	346	465	580
2	41	103	231	352	475	600
6	42	104	234	358	482	610
20	43	105	240	370	500	630
60	44	109	250	382	518	655
600	51	122	278	423	570	720
6000	70	145	330	500	670	820

TABLE 3.1.2B

BEST AVERAGED VALUES OF FORCE VS INDENTATION DEPTH BEHAVIOR OF PMMA AS A FUNCTION OF INDENTATION VELOCITY USING 4.5 mm DIAMETER STEEL INDENTER

Velocity	Load in Pounds at Indicated Depth in mils					
in/min	5	10	20	30	40	50
.0002	51	126	282			
.002	54	134	310	495	675	750
.02	59	146	345	548	752	855
.2	65	163	385	610	835	970
2	74	185	435	681	925	1110
6	79	198	467	723	977	1185
20	86	215	500	771	1035	1260
60	96	240	545	825	1098	1355
600	130	312	675	965	1260	1580
6000	180	405	840	1220	1550	1900

available for PC.) Even this estimate appears to be low. At this stage of our work, there is no clear-cut indication of any limiting upper value for K .

3.2 Force as a Function of Indenter Radius

3.2.1 Experimental. Both from a practical point of view, and for purposes of providing additional insight on the nature of the deformation processes, it is important to know how the size of the indenter affects the response law for the indentation/impact process.

In our measurements, three sizes of spherical indenters were used which differed in radius by a factor of two. These were 2.25 mm, 4.5 mm, and 9.0 mm; and are termed standard, S; medium, M; and large, L. Measurements were made on PC and PMMA at .2 inches/minute and .002 inches/minute indentation velocities up to a load limit of 1000 pounds, which was the capacity of the load cell used.

The results are given in Tables 3.2.1A and B, as well as in Figs. 3.2.1A and B. The data represent the direct test machine results without correction for the machine compliance. This correction is relatively small, is essentially linear with loading, and could be applied at some future time if needed. However, its application is tedious and was judged not to be necessary for purposes of qualitatively examining the effect of size.

3.2.2 Discussion of Results. The scaling of the force response law with indenter geometry is a useful indication of the deformation process. The Meyer[5] law is an empirical law analogous to the Hertz law and can be stated as

$$F = C(r/R)^{n} \cdot R^{2} \qquad (a)$$

in which F is force, r is the radius of the indentation impression, R is the radius of the ball, and C is an experimentally determined empirical constant, having the dimensions of a stress. For ideal

TABLE 3.2.1A

OBSERVED INDENTATION LOADS FOR PC FOR TWO VELOCITIES AND THREE BALL SIZES

Sample Number	Ball	Velocity in/min	$K_o \times 10^{-3}$	Load at Indicated Depth in mils							
				5	10	15	20	25	30	35	40
Ave.*	S	.2	117	40	104		236		366		489
6G	M	.2	137	50	130	222	320	425	530	637	745
7C	"	"	125	45	122	211	310	416	520	629	733
7Q	"	"	135	47	121	210	307	409	510	616	721
Average			132	47	124	214	312	417	520	627	733
5P	L	.2	215	72	192	332	483	639	798	960	
5R	"	"	215	76	197	326	474	640	799	960	
6N	"	"	205	70	189	326	475	632	785	945	
9M	"	"	215	71	191	330	479	639	496	958	
Average			213	72	192	329	478	638	795	956	
Ave.*	S	.002	130	43	104		230		354		475
5M	M	.002	116	41	113	201	292	389	487	583	682
9S	"	"	120	44	120	207	297	390	487	583	678
9W	"	"	125	46	122	211	304	400	498	595	693
Average			120	44	118	206	298	393	491	587	684
4S	L	.002	167	60	168	300	440	590	739	892	
5L	"	"	195	70	186	320	463	613	765	920	
5S	"	"	187	65	180	312	456	605	756	909	
Average			183	65	178	311	453	603	753	907	

*Composite average of previous results.(2)

TABLE 3.2.1B

OBSERVED INDENTATION LOADS FOR PMMA FOR TWO VELOCITIES AND THREE BALL SIZES

Sample Number	Ball	Velocity in/min	$K_o \times 10^{-3}$	Load at Indicated Depth in mils							
				5	10	15	20	25	30	35	40
Ave.*	S	.2	208	65	163		385		610		835
3J	M	.2	175	61	170	302	451	609	770	939	
6D	"	"	191	68	182	319	476	623	789	945	
6M	"	"	215	80	205	347	500	665	830	1000	
Average			194	70	186	323	476	632	796	960	
5K	L	.2	292	100	265	451	648	855			
6E	"	"	321	110	272	460	660	870			
6G	"	"	292	102	263	445	639	837			
Average			302	104	267	452	649	854			
Ave.*	S	.002	166	54	134		310		495		675
7J	M	.002	167	60	157	270	390	516	646	772	900
8G	"	"	167	60	155	270	390	513	641	771	900
8M	"	"	151	53	147	258	377	502	630	757	885
Average			162	58	153	266	386	510	639	767	895
5I	L	.002	245	88	230	389	557	732	911		
7E	"	"	245	88	230	390	561	740	925		
7G	"	"	252	89	227	387	560	740	925		
Average			247	88	229	389	559	737	920		

*Composite average of previous results.[2]

plastic materials, n = 2; for strain hardening materials, n ≈ 2.5; and for elastic materials, n = 3. This law can be recast in terms of the indentation depth x by noting that $r^2 = 2Rx$, to give $F = C'R^2(x/R)^{n/2}$. A more general form is

$$F = C'' x^m R^\alpha \quad . \tag{b}$$

From our extensive studies holding R fixed at 4.5 mm, the value of m has been found to equal 3/2 for small values of x and to decrease for larger values. The value of the other parameter α can now be found from the slope of the log F versus log R curves shown in Figs. 3.2.1A and B. As can be seen, the indentation force in the case of the small and medium indenters at small indentation depths was insensitive to size in the case of PC and PMMA at both velocities. Thus, the Meyer law does not appear to be a good representation of the material behavior in this regime, although it does describe the data well at the greater depths. The values for the standard indenter were those obtained in our previous study,[2] whereas the present results for the M and L indenters were obtained in a single set of consecutive experiments in which the indenter was changed, but the rest of the setup remained fixed. We do not believe that combining the older data with the new could account for the observed lack of dependence of force on the indenter size at small depths, because the required force to be consistent with the Meyer law would be substantially beyond experimental error.

If the best straight lines are drawn through the data, then the value of α is found to increase with increasing depth. These results are shown in Table 3.2.2A.

Physically, one expects C'' in Eq. (b) to have the dimensions of a stress (or elastic modulus). For the Hertz law, C'' is identified with the Young's modulus; for ideal plastic solids, C'' is identified with the yield stress. Therefore, on dimensional grounds, we require

TABLE 3.2.2A

DEPENDENCE* ON INDENTATION FORCE ON BALL RADIUS
FOR PC AND PMMA AT .002 AND .2 INCHES/MINUTE

	PC			
x (mils)	Velocity	α	Velocity	α
5	.002	.30	.2	.42
10	"	.40	"	.45
20	"	.50	"	.57
30	"	.56	"	.55
	PMMA			
5	"	.32	"	.28
10	"	.35	"	.29
20	"	.41	"	.33
30	"	.44	"	---

*$F = K(x) \cdot R^{\alpha}$

$$F = C'' R^2 (x/R)^m \quad , \qquad (c)$$

so that $\alpha = 2-m$. As discussed $m = 3/2$ for small x and approaches 1 for large x. Therefore, α is expected to vary from .5 to 1 over the same range of depth. Comparison with the table shows α to range from about 0.3 to 0.55. The reason for this is not understood at this time, but probably signifies that a mix of basic processes is occurring simultaneously.

3.3 Force Relaxation

3.3.1 Experimental. In order to determine directly the effect of time on the response behavior from that of increasing the penetration depth, measurements were made on the decay of the force as a function of time when the indenter is held stationary. The procedure was simply to force the indenter into the specimen at a selected constant velocity, to stop the machine at a desired depth, and to follow the decay of the force as sensed by the load cell. Typically, the period of relaxation was comparable to the time required for the indenter to penetrate to the depth of concern. In some cases at the conclusion of the relaxation, observations at a given depth, the indentation was continued and the process repeated. In this way relaxation could be studied at several depths in the same specimen. It was experimentally found that stepwise loading gave equivalent results to loading without interruption to the same depth, providing that the indenter travels between steps was sufficiently large.

As will be discussed in the next section, it has been found that the following empirical equation represents the data very closely over the entire range of the observations:

$$F(t)/F(o) = (1+AT)^{-B} \quad ,$$

in which F(t) is the force at the time t indicated, and A and B are experimentally determined constants. The results of measurements on PC and PMMA are given in Tables 3.3.1A and B for indentation depths of 10, 20, 30, and 40 mils, at rates of .002 and .2 inches/minute, and using the standard (4.5 mm) and large (18 mm) diameter indenters. Table 3.3.1C gives the results on another series of measurements on PMMA made following the conclusion of complete force-indentation runs to depths of 50-100 mils, using the standard indenter. These results cover the velocity range from .002 to 20 inches/minute.

3.3.2 Discussion of Results. Knowledge of the relaxation behavior is important to extrapolate the stress and stress relaxation rate back to zero time, as well as providing insight into the nature of the relaxation process. Classically, one expects the stress σ (at fixed strain) as a function of time to follow

$$\sigma(t) = \sum_i A_i \, e^{-t/t_i} \qquad \text{(a)}$$

where t_i and A_i describe the spectrum of relaxation times and amplitudes, respectively. This has the property that $\sigma_{(o)}$ is finite when t = 0. The simplest case would be when there is only one relaxation time, i.e.,

$$\sigma(t) = \sigma_{(o)} \, e^{-t/t_o} \quad . \qquad \text{(b)}$$

Analysis of the relaxation results showed that this kind of expression does not fit the data well, because it results in a much too rapidly decaying force behavior. (This was true as well for the modified form (b') shown below.) Several empirical functions were examined. These included:

$$F(t) = F(o) \; [(1-A_1)\exp(-B_1 t) + A_1] \qquad \text{(b')}$$

TABLE 3.3.1A

CHARACTERISTIC RELAXATION PARAMETERS FOR PC AS A FUNCTION OF VELOCITY, DEPTH, AND INDENTER SIZE

Sample Number	Velocity in/min	Ball	x mils	A	B	A·B
1U	.002	S	10	7.36	.031	.23
10H				8.80	.028	.25
1U	"	"	20	5.58	.038	.21
2P				6.79	.036	.24
10H				4.36	.037	.16
1U	"	"	30	4.33	.044	.19
10H				3.42	.042	.14
1U	"	"	40	4.08	.045	.18
2K				3.86	.046	.18
10H				4.40	.039	.17
10Q	"	L	10	2.34	.022	.051
			20	2.11	.023	.049
			30	2.58	.025	.065
			40	2.75	.027	.074
10G	.2	S	10	505	.026	13.1
			20	565	.030	17.0
			30	690	.034	25.3
			40	417	.038	15.8
10B	"	L	10	563	.011	6.2
			20	230	.018	4.1
			30	204	.022	4.5
			40	188	.025	4.7

TABLE 3.3.1B

CHARACTERISTIC RELAXATION PARAMETERS FOR PMMA AS A FUNCTION OF VELOCITY, DEPTH, AND INDENTER SIZE

Sample Number	Velocity in/min	Ball	x mils	A	B	A·B
5F	.002	S	10	3.22	.068	.22
13Q				3.74	.067	.25
5F	"	"	20	2.33	.081	.19
5G				2.29	.082	.19
13Q				3.55	.069	.25
5F	"	"	30	1.66	.093	.15
13Q				1.61	.090	.15
3C	"	"	40	1.42	.098	.14
5F				1.59	.094	.15
13Q				2.00	.085	.17
10P	"	L	10	1.43	.052	.074
			20	1.43	.051	.073
			30	1.08	.057	.062
			40	0.91	.063	.057
10E	.2	S	10	274	.064	17.5
			20	154	.070	10.8
			30	220	.078	17.2
			40	83	.086	7.1
9H	"	L	10	154	.043	6.6
			20	105	.048	5.0
			30	39.2	.052	2.0
			40	19.8	.056	1.1

TABLE 3.3.1C

CHARACTERISTIC RELAXATION PARAMETERS FOR PMMA AS A FUNCTION OF VELOCITY AT LARGE INDENTATION DEPTHS

Sample Number	Velocity in/min	x mils	F(o) lbs	A	B	A·B
224	20	45	1176	12273	.1067	1310
226	20	50	1266	14288	.0980	1400
227	20	45	1168	10227	.1089	1110
232	2	55	1240	977	.1203	118
233	2	60	1384	1245	.1004	125
236	2	60	1320	1152	.1098	127
240	.2	70	1376	115.9	.1058	12.3
241	.2	70	1400	140.3	.0978	13.7
242	.2	70	1372	100.0	.1249	12.5
219	.02	100	1928	8.25	.1004	.83
220	.02	100	1976	7.59	.1078	.82
210	.002	110	1670	0.889	.1055	.094
211	.002	110	1700	0.905	.1074	.097

$$F(t) = F(o) - \frac{B_2 t}{1+A_2 t} \qquad (c)$$

$$F(t) = F(o) - B_3 \ln (1+A_3 t) \qquad (d)$$

$$F(t) = F(o) - B_4 \frac{\ln (1+A_4 t)}{\ln (1+C_4 t)} \qquad (e)$$

and

$$F(t) = F(o) (1+At)^{-B} \qquad (f)$$

The parametric equations (b'), (c), and (d) were less successful than were equations (e) and (f). For very long times, (e) leads to a finite residual force, whereas (f) leads to complete relaxation. However, over the range of the observed times, there is little to choose between them. We have accordingly adopted the latter representation, not only because it is the simpler expression, but also it appeared to be the more exact. A comparison of the results is given below for the case of the relaxation of PMMA indented at .002 inches/minute to a depth of 110 mils.

Equation	A	B	C	% Error
b'	.745	.222	----	2.0
c	.29	150	----	7.2
d	1.35	137	----	2.0
e	1.26	141.7	.001	2.0
f	.905	-.107	----	0.1

The values of the A and B parameters, listed in the tables in the preceding section, were computed using the Fletcher-Powell method which minimizes the overall error. The results for both materials corresponding to indentation velocities of .002 and

.2 inches/minute and for the standard and large indenter are displayed in Figs. 3.3.2A to D. These show that the parameter B is insensitive to velocity but increases with increasing depth for both size indenters. It is a function of ball size, decreasing with increasing ball size. The behavior of A is more complicated. Generally speaking, A appears to decrease with increasing depth, the effect being larger for the higher velocity. There appears to be no simple scaling with indenter size. However, the most remarkable, and apparently quite general, behavior is the nearly exact proportionality between the velocity and the value of A, as is shown in Fig. 3.3.2E. $A \approx ku$, where k is a constant. The initial rate of stress decay is given differentiation of Eq. (f) to give:

$$(\partial F/\partial t)_x = -F(o)\ A \cdot B = -F(o)\ kuB \quad .$$

Now, in a constant velocity experiment, this represents the rate at which the stress is relaxaing while the penetration is proceeding. Expressing this mathematically, during an interval of time dt in which the indenter is advancing a distance u dt = dx, the increase in force is given by:

$$dF = \left(\frac{\partial F}{\partial t}\right)_x dt + \left(\frac{\partial F}{\partial x}\right)_t dx$$

$$\text{or} \quad \frac{dF}{dx} = \left(\frac{\partial F}{\partial t}\right)_x \Big/ u + \left(\frac{\partial F}{\partial x}\right)_t$$

$$= - FkB + \left(\frac{\partial F}{\partial x}\right)_t \quad .$$

Since k and B are weak functions of velocity, the effect of the relaxation on the force-indentation behavior is relatively insensitive to velocity. This is so in spite of a very substantial and sensitive intrinsic dependence of the force on time.

The physical significance of the various terms is illustrated in Fig. 3.3.2F, which shows an actual trace of the force behavior of PMMA being indented at .002 inches/minute when the process is abruptly stopped at 10 mils penetration. The decay in the load is followed for five minutes, and then the indentation is allowed to proceed. The various portions of the curve are labeled. Strictly speaking, the slope that first appears on restarting the indentation is not exactly the same as $(\partial F/\partial x)_{t=0}$, which corresponds to "infinitely fast" loading. The corresponding information on PC and PMMA obtained from these interrupted loading experiments has been analyzed, and the results are shown in Table 3.3.2A. The calculated values for $(\partial F/\partial t)/u$ are derived from information in Figs. 3.3.2A and C in conjunction with the measured values of dF/dx and F corresponding to the particular sample. The predicted slopes for startup after stopping the process generally agree within 20% of the observed values but, surprisingly, consistently underestimate the "hardness."

Finally, it is of interest to estimate the relative importance of the relaxation term to the corresponding "instantaneous" loading term. For the general case, this is most conveniently done by making use of Figs. 3.1.2E and F to obtain F and dF/dx, and using Figs. 3.3.2A and C to obtain A and B. We show in Table 3.3.2B the representative results for PC and PMMA using the standard indenter for velocities of .002 and .2 inches/minute. This shows that the relaxation is a very important term at all stages of the indentation, and increasingly so as the depth increases. This strong time-dependence means that the actual load-, depth-time response will probably be path dependent.

TABLE 3.3.2A

COMPARISON OF OBSERVED AND CALCULATED LOAD COMPONENTS IN PC AND PMMA AT .002 IN/MIN INDENTATION VELOCITY

x mils	F lbs	AB/u	dF/dx (= net loading rate)	(∂F/∂t)/u (= relaxation component)		∂F/∂x (= instantaneous loading component)	
			ksi/in				
			obs.(a)	calc.	obs.(b)	calc.*	obs.
			PC				
10	105	88	12	9	15	26	29
20	240	94	12	19	20	32	39
30	370	90	12	33	27	39	46
			PMMA				
10	140	117	16	16	15	30	42
20	320	85	19	27	24	42	46
30	510	70	15	36	36	51	57

*This column is the sum of the columns marked (a) and (b).

TABLE 3.3.2B

ESTIMATE OF MAGNITUDE OF RELAXATION VS INSTANTANEOUS LOADING TERMS FOR PC AND PMMA

Velocity in/min	x mils	F	dF/dx	$(\partial F/\partial t)_x/u$	$(\partial F/\partial x)_{t=0}$
				ksi/in	
			PC		
.002	10	100	13	8.8	22
	18.5	200	"	19.5	32.5
	27	300	"	28.5	41.5
	35	400	"	36	49
.2			SAME		
			PMMA		
.002	8	100	18.3	12	30
	13.5	200	"	22	40
	19	300	"	30.6	49
	25	400	"	37	55
.2	7	100	22.3	12	34
	11.5	200	"	23	45
	16	300	"	32.25	55
	20.5	400	"	40	62

3.4 Rate Change Tests

3.4.1 Discontinuous Change in Velocity. Indentation tests during which the rate was changed during the test were performed on both PMMA and PC. The purpose of these tests was to determine how well the phenomenological equations, developed to express the deformation behavior of PMMA and PC (described in Section 3.1.1) under constant rate conditions, described indentation behavior under such conditions.

The tests were performed in an Instron machine using the standard 4.5 mm indenter. The two deformation rates employed were .002 and .02 inches/minute. These rates were chosen in order to obtain a two order of magnitude rate change and still remain within the recording capability of the Instron recorder. The procedure was to indent to a depth of .010 inches at the slow rate, change the rate 100-fold by changing the Instron clutch position, and impress an additional .010 inches, change back to the slow rate for the next .010 inches, and so on until a total depth of .050 inches was reached. The chart speed was not changed; magnification of 1000 and 10 were obtained at the slow and fast speed, respectively.

The data are shown in Figs. 3.4.1A and B for PMMA and PC. The solid lines expressing the predicted results from the equations will be discussed in Section 4.1. It may be noted that the increments for PC were not .010 inches due to operator error. This is not considered a serious deficiency. The behavior on load change is the same for both materials but is more pronounced and can be seen better for PMMA. When the rate was changed, considerable time was required by the material to stabilize at its new rate. Stress relaxation occurs when the rate is abruptly slowed, as can be seen by the load decrease followed by a load increase to approach the new steady state rate. These effects become more pronounced as the deformation increases, suggesting the volume of deformed material is of importance. The behavior is quite complex; and for its complete description, a detailed visco/elastic/plastic analysis would be required.

3.4.2 Continuous Change in Velocity. Several tests were performed in the MTS machine using a sinusoidal indentation mode in which the ram of the testing machine was programmed to move through one full sine cycle. The specimen was positioned so the indenter was just in contact with the specimen. The ram first went up, contacted the specimen midway through the period, indented during the third quarter of the cycle, and unloaded during the last quarter. It may be seen that during the indentation quarter of the cycle, the ram velocity was initially constant, then slowed down and decreased to zero. In this respect the motion simulates a free particle impact with the polymer surface in that its velocity is initially constant and subject to increasing deceleration, until the velocity is finally zero. During deceleration of the free particle, the motion will be more complicated than a simple sinusoid. Nevertheless, it was felt that if the deformation behavior could be approximately predicted using equations, such as those developed in Sections 4.1 and 4.2, then a start would have been made in understanding the material response to ballistic impact.

These equations predict the force response as follows. The equations in Section 4.1 are of the form

$$F = Au^m x^n \quad . \tag{a}$$

Under sinosoidal loading, the deflection x is given by

$$x = K \sin bt \qquad \frac{\pi}{b} \leq t < \frac{3\pi}{b} \tag{b}$$

where t is the time, $3\pi/b$ the period, and K the amplitude. Differentiation (b) gives the velocity u

$$u = \frac{dx}{dt} = Kb \cos bt \tag{c}$$

sc

$$F = A\ (Kb \cos bt)^m\ (K \sin bt)^n \qquad (d)$$

or $$F = AK^{m+n}\ b^m\ (\sin bt)^n\ (\cos bt)^m \qquad (e)$$

Several tests were performed on both PMMA and Lexan, with a typical load deflection curve shown in Fig. 3.4.2A. When attempts were made to fit the data using the equations in Section 4.1, a factor of two discrepancy between observed and predicted load was obtained. We suspect that an incorrect machine calibration was used, but because of the heavy demand on this machine, we have not yet had an opportunity to perform an independent calibration.

3.5 Microindentation Hardness Measurements

Occasionally in measuring the force-indentation behavior for PC and PMMA, an anomalous result occurs which markedly departs from those derived from nominally identical specimens. In order to try to characterize the mechanical homogeneity of the materials, diamond pyramid hardness measurements were made on some representative specimens. A standard load of 25 g was applied at a rate of about .07 inches/minute = .03 mm/second and was allowed to come to rest for 10 seconds. Nine measurements were made on nominally identical 1" x 1" samples at x coordinate positions of .150, .400, and .525 inches from a reference edge, and at y coordinate positions of .3, .6, and .9 from the other edge. The specimens were coated with evaporated aluminum, and the lengths of the diagonals of the pyramid impression were measured using a micrometer eyepiece. The units of length in Figs. 3.5A and B for PC and PMMA, respectively, are the micrometer readings and are reproducible to ±0.5 units. Differences greater than 1 in the readings, therefore, are considered to be significant. The data for PC indicate normal

distribution of values having a standard deviation of 1.6%. However, the results for PMMA are unusual in that the distribution appears to be bimodal. About .4 of the measurements are grouped around a mean value of 64 with a standard error of 4% and .6 of the values are grouped around a mean of 76.6 also with a standard error of 4%.

It is instructive to note the variation along a given row, in the case of PMMA, in which numerous microindentations were made at close distances in order to investigate the scale in which significant materials variation might occur.

Distance in inches	.350	.375	.400	.412	.425	.45	.525
Indentation Size	66	63	58	62	72	67	66

This is a marked variation on the scale of .010 inches. It is not known whether this represented an unusual "knot" in the material or what the distribution of such anomalies might be. In any case the result is unexpected. A priori we would expect the cast material (PMMA) to have higher reproducibility than the extruded material (PC). The fact that these variations occurred on a relatively fine scale within an individual block suggests that variations in the force-indentation response must be expected in measurements on commercial material.

3.6 Physical and Geometric Characterization of the Crater Region

Whereas the force-indentation measurements are basic to the mechanics of the impact response, they are only indirect clues of the actual physical processes that determine that response. Accordingly, we have also been concerned with a more direct study of the deformed zone that results from impact (indentation). Viscous and plastic flow are by their nature nonrecoverable, elastic response is instantaneously recoverable, and anelastic response can be frozen in, but recovered with time and annealing. It is of interest to understand how a rapid nonelastic response can occur in

materials, such as PMMA, PC, and epoxy which are far below their transition temperatures for plastic flow (Tg). These are the matters of major concern in this section.

3.6.1 Experimental. Generally there is a region of material having an altered appearance that lies directly under an indentation crater. This material is transparent but is optically distinguishable presumably having a different refractive index or birefringent properties from the undisturbed material. This becomes noticeable when the specimens are polished on their side so that the interior of the sample can be viewed. Figs. 3.6.1A-C show typical cases for PC, PMMA, and epoxy. These regions are difficult to see and require special lighting conditions.

Some preliminary annealing experiments were done on PC specimens which had been subjected to deep indentations. At 145°C, as measured by the depth of the crater, 40% recovery had occurred in one hour, and virtually total recovery was noted after 50 hours, as is shown below.

Anneal Time	Depth and Specimen Designation		
	5J	4M	6L
0	.005	.044	.108
1	0	.025	.060
50	0	0	.004

Specimen 6L contained a crack, which apparently perturbed the stress field sufficiently to prevent complete recovery. In the case of 4M, after the anneal there was no sign of the specimen having been indented, nor was any trace of disturbed material detectable under ordinary or polarized light inspection.

Except for the measurements involving the high velocity ballistic impacts, the observations were intended to cover a wide range of

conditions and materials, rather than to be a systematic investigation. The results for these typical cases are shown in Table 3.6.1A. The results for the ballistic impact studies are given in Table 3.6.1B. Except where the examination is obscured by cracking, such as occurs at the higher velocities in the case of PMMA, the distrubed zone can be reproducibly measured to about .01 inches. Specimens which had previously been used for indentation-force measurements were used for these present studies. In addition a series of craters was produced in PC and PMMA by firing 4.5 mm projectiles at velocities from ca. 400-750 feet/second using a compressed air gun. In another test, a piece of PC was cooled to 78°C before impacting a 4.5 mm ball placed on its surface with a hammer. The estimated impact velocity in this case was 30 feet/second.

The dimensions of the craters and the disturbed zone were measured as indicated schematically in Fig. 3.6.1D. The disturbed zone was measured by sighting transversely through the specimen under suitable lighting conditions, holding the specimen at a distance to minimize parallax, and using the jaw opening in a vernier caliper to gage the size. An average of three to five measurements was used to define each geometric quantity.

Finally, to establish whether densification may be associated with the "disturbed" regions, the density of this material was determined by carefully sawing out small blocks of material from under the crater. Care was taken to keep the saw blade lubricated with water so as to avoid heating. The blocks, roughly 3 mm on an edge were placed in a density gradient column, and their density determined by floatation. This technique involves placing a solution of potassium iodide in a large graduated cylinder. The solution is made to be more concentrated at the bottom and to become progressively more dilute linearly with increasing height. Hence, an object placed in the gradient column will sink to a level such that the density of the solution is equal to its own. The material underneath the crater reached a point of neutral buoyancy, lower in the column, than did the undisturbed material. This can be seen in Fig. 3.6.1E. The

TABLE 3.6.1A

GEOMETRIC PARAMETERS CHARACTERIZING IMPACTED REGION FOR PC, PMMA, AND EPOXY

	Crater Geometry						Disturbed Zone Geometry			
Specimen	2R in	2a in	$x_{obs.}$ in	$x_{calc.}$ in	$x_{max.}$ in	V_c $x10^4 in^3$	2r in	h in	V_z $x10^3 in^3$	V_z/V_c
					PC (R.T.)					
7B	.177	.15	.05	.042	---	564	.33	.27	17.2	30
9S	.354	.220	.020	.036	.040	8.8	.29	.21	10.4	11.8
5S	.709	.198	.003	.026	.035	14.0	.21	.14	3.6	2.56
					PC (78°C)					
6J	.177	.124	.005	.023	---	1.43	.16	.08	1.1	7.5
					PMMA (R.T.)					
1M	.177	.100	.005	.014	.020	0.55	.11	.07	.49	8.9
8D	"	.177	.056	.088	---	8.9	.35	.20	13.6	15.4
					EPOXY (R.T.)					
1	.177	.127	.012	.025	---	1.7	.21	.12	2.9	17.5

TABLE 3.6.1B

GEOMETRIC PARAMETERS CHARACTERIZING IMPACTED REGION FOR PC AND PMMA RESULTING FROM BEING STRUCK BY .177 INCH DIAMETER PROJECTILES

	Crater Geometry				Disturbed Zone Geometry			
Velocity ft/sec	2a in	$x_{obs.}$ in	$x_{calc.}$ in	V_c $x10^4 in^3$	2r in	h in	V_z $x10^3 in^3$	V_z/V_c
				PC				
442	.148	.0105	.036	3.33	.210	.125	3.11	9.3
436	.159	.0156	.044	4.79	.215	.130	3.41	7.1
616	.174	.0184	.058	7.99	.235	.145	4.51	5.7
682	.175	.0193	.060	8.27	.245	.160	5.56	6.7
746	.175	.0210	.060	"	.265	.185	7.62	9.2
				PMMA				
550	.141	~0	.032	2.65	.135	.089	9.42	3.6
624	"	"	"	"	"	.101	"	"
690	"	"	"	"	.140	.100	"	"
763	"	"	.039	3.62	*	*	*	*

*No measurement possible because of cracking.

three lower blocks are indented PC, whereas the top three blocks are in normal material. The density gradient was established to be .00206 $(g/cm^3)/cm$. Since there is about 1 cm difference in height between the lowest and highest pieces, the density increase is about .002 g/cm^3. This corresponds to a 0.16% relative change in density. The measurements on PMMA were inconclusive because the gradient column gradually becomes unstable due to mixing (inserting and removing specimens) and due to thermal mixing. Setting up such a column is a tedious, lengthy process. A second column was not set up because the phenomena seemed to be the same for the cases of PC, PMMA, and epoxy as evidenced by their optical appearance.

3.6.2 Discussion. The above results are noteworthy in terms of their apparent generality. The "disturbed" zone can apparently be interpreted as a densified zone, and this densification is anelastic in nature. That is, it is recoverable with long time, and/or annealing. This is quite contrary to the concept of viscoelastic behavior and corresponds more closely to elastic-plastic behavior, except that the plastic part is really anelastic.

It has been shown that the surfaces representing constant yield stress as based on the vonMises criterion follow roughly hemispherical contours. This is seen in Fig. 3.6.2A. The parallelism between this and the observed densification zone is obvious. Typically, the results for PC, PMMA, and epoxy show that the depth of the yield zone extends into the material a distance approximately equal to the diameter of the indentation crater. This might at first sight suggest that the yield stress is about .12 times the maximum stress under the indenter. However, this can only be interpreted as a lower bound because the stresses within the densified region will not be given by the elastic analysis. Nevertheless, the tendency for a spherical like yield behavior can be expected. This will be discussed further in Section 4.

The fact of the density increase observed for PC is perhaps to be expected. However, the absolute magnitude of the increase is only about 10% of what was expected on the basis of the volume of the residual densified zone, relative to the volume of the crater. Elastic deformation and piling up of material around the crater edge may account for some of the discrepancy. In addition, further anelastic recovery can be expected to occur when the constraint provided by the mass of the remaining material is removed.

4. MODELING AND ANALYSIS

This chapter is concerned with developing predictive models and expressions of the material response. The experiments have been mainly performed under conditions of constant velocity. However, ballistic impact encounters due to a collision with a flying object results in rapid decelerations and consequently a much more complex time-velocity-displacement history. Hence, some approach to dealing with this situation is needed. The section that immediately follows is a model, similar to metallurgical models in which the stress is related to a function of the instantaneous strain and strain rate. This is followed by another type of model, which attempts to relate the results of the relaxation measurements to the force response of the indenter. Finally, there is an attempt to model the impact process as an elastic-plastic deformation process. Each has a certain degree of success and deficiency as will be shown.

4.1 Phenomenological Model of Indentation Process

4.1.1 Description of Model. The data obtained from the indentation experiments performed to date will be ultimately used to analyze and predict ballistic impact tests. Here the loading history is far from simple, and methods must be developed to account for these changed loading conditions.

Theoretical modeling of the response is already a complex problem for the case of linear viscoelastic materials subjected to simple stresses. It is further complicated in the current case because of the combined (and changing) stress state in the indentation process. Although viscoelastic stress analysis is possible,[6] it is time consuming and requires uniaxial material properties to define the relaxation spectrum that are not available for the PMMA and PC used for the current tests. Consequently, a far simpler approach will be used.

It has been shown for metals[5] that the applied force F is related to the displacement x in hardness tests by a relation of the form

$$F = Kx^m \qquad (a)$$

This is only approximately true for metals and is probably incorrect for polymers. Nevertheless, a plot of log x versus log F at a particular rate yields an approximately straight line, and the lines of log F versus log x are approximately parallel for different rates. As a starting point, and with the full knowledge that the resulting equations are only crude approximations, the average deformation data were fitted to an expression of the form

$$F = Ku^n x^m \qquad (b)$$

The ability of these equations to predict the experimental results was examined, and their utility to predict rate-change data examined.

The equations derived to represent the force-indentation rate relation for PC and PMMA are as follows:

$$F = 34670\, u^{.0596}\, x^{1.143} \quad \text{(PMMA)} \qquad (c)$$

$$F = 23380\, u^{.0290}\, x^{1.187} \quad \text{(PC)} \qquad (d)$$

PMMA showed a better fit than PC, and PC showed a somewhat better fit when m instead of being constant was assumed to have the form

$$m = K_2\, u^{n2} \qquad (e)$$

However, the fit was only marginally better; because it is of interest to compare the derived material parameters A, m, and u for PMMA and PC, the less complicated form was used.

The ability of these equations to predict the original data is shown in Figs. 3.1.2A and B. The maximum error is of the order of 20%, which is the same order as the experimental scatter. PC seems to show less conformity to the data than PMMA, but the load scale is twice that of the PMMA.

Examination of Eq. (c) and (d) indicates clearly the quantitative differences in the response of PMMA and PC to indentation. The strength coefficient, A, is 48% greater for PMMA, representing the greater resistance to indentation of PMMA. The rate exponent, m, for PMMA is about twice that of PC, indicating the former material is much more rate sensitive than the latter. This is evident from an inspection of the data. On the other hand, the relation between force and displacement at a particular rate is about the same, as evidenced by the similar values of the deformation exponent, n.

It may be seen, then, that for constant displacement indentation tests and for finite displacement greater than, say, several mils, the behavior of PMMA and PC can be fairly well approximated over about eight orders of magnitude in rate by a simple expression. How well these equations will predict behavior under more complicated loading histories will be examined in the next section.

4.1.2 Discussion of the Model. In Section 3.4.1, data are reported in the material response of PC and PMMA to repeated rate changes between .002 and .02 inches/minute. Shown on Figs. 3.1.1A and B are the predicted behavior based on the two equations described in the previous section. Reference to these figures shows that indeed the equations do envelop the data within the 20% derived accuracy. However, it is clear that the material behavior is more complex than that described by an equation of the form $F = Au^m x^n$. If the material obeyed such a law, instantaneous rate changes would

produce abrupt load increases and decreases. This does not occur, and rate changes result in complicated transient responses. Nevertheless, the fact that we can predict in general the deformation to within 20%, although certainly not the details, gives some hope that the approach can at least be used as a first approximation to the ballistic impact problem.

4.2 Force Relaxation Law

4.2.1 Relationship Between Force Relaxation Law and Basic Molecular Relaxation.

The force relaxation behavior as described in Section 3.4 already represents a complex situation. In a constant velocity experiment, force and deformation increase steadily until at some point the process is halted and observation of the relaxation is initiated. At this instant the time is set equal to zero. However, stress relaxation has been occurring ever since contact was first made with the indenter. Hence, the force at time t = 0 is a partially relaxed force. This situation is illustrated in Fig. 4.2.1A.

Our objective in this section is to try to relate the observed law to the more fundamental law which describes the relaxation that is going on continuously. Defining Region I as the force response during the period in which the loading is taking place, and Region II as the relaxation during the time period in which loading is stopped. The stress behavior can be qualitatively expressed by

$$F = \underbrace{\int_0^{\tau} (\partial F/\partial x)_u \, u \, dt}_{\text{Region I}} + \underbrace{\int_{\tau}^{t} (\partial F/\partial t)_x \, dt}_{\text{Region II}} \qquad \text{(a)}$$

in which time t is now measured from the instant of first contact between the indenter and the material, τ is the time at which the indenter is stopped, u is the indentation velocity, and F is force.

Region I does not concern us at this time. In principle, it is possible to arrive at the basic relaxation law $F = F(o) \cdot g(t)$ by solving the following equation for g:

$$F(t, x = \text{constant} = x_o) = \int_o^{x_o} f(x)\, g(t - \frac{x}{u})dx \quad , \qquad (b)$$

in which f(x) is the time independent (i.e., infinitely fast) dependence of force on incremental indentation depth, and $F(t, x_o)$ is the observed relaxation.

This integral is called an involution integral and can be solved using LaPlace transforms providing that f(x) is known.

4.2.1.1 Behavior at Small Indentation Depths. One of the immediate questions of interest is whether Eq. (b) in the above section could explain the fact that experimentally at small indentation depths the force is proportional to $x^{3/2}$, but that the proportionality constant depends on u and is not simply related to the elastic modulus. To test this, we set

$$f(x) = \frac{d}{dx} K_{el}\, x^{3/2}$$

where K_{el} is the Hertz constant for the strictly elastic case. In effect Eq. (b) above states that at every instant of the deformation material is being transformed into a stressed state and that relaxation from that state starts immediately. Some kind of model is needed to define whether that new stress state is being created proportionally to the new volume displaced, the new surface, to the total volume, etc.

It is straightforward* to show that there is no weighting function w(x) which can lead to the result

$$K'(ut_1)^{3/2} = \int_o^{t_1} w(x) \cdot f(x) \cdot g(t_1 - t)\, dt$$

for small values of t, such that K' ≠ K elastic.

We must conclude, therefore, that either the force as a function of depth was not carried out in a small enough depth range to lead to the correct elastic modulus, or that this kind of distributed relaxation model is inappropriate. Since, even the measurements at small depths with large diameter balls did not lead to a measured value of K' that corresponded to the elastic value, it appears that the second alternative is probably correct. Hence, at this time, it is not clear as to what basic information can be derived from experiments at small depths.

---

* Let $w(x) = a_1 x^n = a_1 (ut)^n$.

$$f(x) = (3/2) \cdot K_{el} (ut)^{1/2} \quad .$$

or $$K' u^{3/2} t_1^{3/2} = (a \cdot u^{n+1/2} \cdot 3/2K_{el}) \int_o^{t_1} t^{n+1/2}\, g(t_1 - t)\, dt \quad .$$

Defining $A = 2K'u/3au^n K_{el}$ and taking LaPlace transforms of both sides gives

$$A \cdot L\{t_1^{3/2}\} = L\{t_1^{n+1/2}\} \cdot L\{g\} \quad .$$

Note: $$L\{t^n\} = \frac{n!}{s^{n+1}}$$

$$\therefore \quad L\{g\} = A \frac{(3/2)!}{s^{5/2}} \Big/ \frac{(n+1/2)!}{s^{n+3/2}}$$

$$= A \left[(3/2!/(n+1/2)!\right] / s^{1-n} \quad \text{or} \quad g = \frac{A(3/2)! t^{-n}}{(n=1/2)!(-n)!} \quad .$$

Since the relaxation function g = 1 at zero time, the only solution possible is n = 0, or $K' = K_{el}$.

4.2.1.2 Relaxation Following Sudden Halt of Constant Velocity Indentation. When the indentation is abruptly halted at large depths, relaxation can be followed, and Section 3.3 has presented information showing that $F = F(o)\ (1+A\tau)^{-B}$ is an excellent representation of such relaxation. We have purposely used τ to represent time since relaxation had been previously occurring as already discussed. In order to get at the intrinsic relaxation law (in contrast to the net relaxation which is actually observed), it is necessary to use an expression similar to Eq. 4.2.1(b). We assume that indentation proceeds at the constant rate u up to a time t_o at which time the indenter is halted and observation of the relaxation process commences. At this point a second clock is started which measures the time interval τ starting at t_o. Therefore, the relaxation after time t_o is represented by

$$F(\tau) = \int_o^{t_o} f(x)\ g(t_o + \tau - t)\ dt \qquad (a)$$

in which $F(\tau)$ is the observed relaxation. This is a very complex equation to solve. It is instructive to consider the hypothetical case in which the intrinsic relaxation law is known and is $g(x) = e^{-\beta x}$. Then, let

$$f(x) = \frac{3}{2} K_{el}\ x^{1/2} \quad .$$

This gives

$$F(\tau) = \frac{3}{2} K_{el}\ u^{3/2}\ (e^{-\beta t_o} \int t^{1/2}\ e^{\beta t}\ dt)\ e^{-\beta t} \qquad (b)$$

$$= F(t_o)\ e^{-\beta t}$$

$$= F(\tau = 0)\ e^{-\beta \tau}$$

Thus, the net relaxation law and the intrinsic law are identical.

We have carried out a similar type of analysis, knowing that

$$F(\tau) = F(\tau = 0)\ (1+A\tau)^{-B},$$

using an expression that parallels (b), namely,

$$F(\tau =0)\cdot(1+A\tau)^{-B} = \frac{3}{2} K_{el}\ u^{3/2} \int_{o}^{t_o} t^{1/2}\ (1+a[t_o+\tau-t])^{-B}\ dt \qquad (c)$$

and trying to solve for a. This is no longer separable into distinct factors as in case (b). The integral on the right can be reduced to a standard form known as an incomplete beta function, many of the properties of which are known. Working with the integral does indeed lead to a solution of the form

$$F(\tau) \approx F(\tau=0)\ (1+a\tau)^{-B}$$

where $a = \frac{A}{1-At_o}$, provided $At_o << 1$.

4.2.1.3 Extension to More Complex Systems. Having some reasonable assurance that the intrinsic relaxation function can be reasonably approximated by the net relaxation function, an attempt was made to consider the case of an abrupt change in velocity, in which the incremental increase in the force was assumed to decay away at a rate characteristic of the velocity at the instant that the force increase occurred. This is a difficult analysis and is not complete at this time. However, the results qualitatively can be anticipated to be at variance with experiment in the sense that a monotonic transition from one state to the other will result. The experiments show that overshoot occurs either when velocity is abruptly increased or decreased. This is then followed by an asymptotic drift towards the uninterrupted constant velocity values.

4.3 The Plastic-Elastic Model

Among the more prominent features of indentation response are (1) the nearly linear increase of load with penetration depth for both PC and PMMA over a wide range of velocities and depths, and (2) the very large volume of densified (or yielded) material that lies directly beneath the indentation and that assumes the form of a truncated sphere.

Considering the yielded material to be in a state of hydrostatic compression leads to the following expression for the force on the indenter:

$$F = \pi a^2 p$$

in which a is the radius of the indentation and p is pressure. Since for small depths, $a^2 \approx 2xR$, it follows that $F = (2\pi Rp)x$. If p is constant, then the observed behavior is predicted. The slope dF/dx can be used to measure p. Following Hill's treatment[7] of the plastic yielding of a spherical cavity in an infinite medium

$$p = \frac{2Y}{3}\left(1+\ln\frac{E}{3(1+\nu)}\right)$$

where Y is the yield stress, E is the Young's modulus, and ν is the Poisson ratio for the material. Thus, p is a unique function of Y and is predicted to be constant during the course of the plastic deformation. Therefore, making use of the slopes in Figs. 3.1.2E and F as well as typical values for the Young's modulus of PC and PMMA of 350,000 and 420,000 psi, respectively, and taking ν for both polymers to be ca. .35, the following results are obtained for the estimated pressure and yield stress:

	Velocity in/min	dF/dx ksi/in	p ksi	Y ksi	Y/E
PC	.002	13	11	3.3	.009
	.2	13	11	3.3	"
PMMA	.002	18.3	15.5	4.9	.012
	.2	22.3	18.9	7.7	.018

Another measure of the yield stress is possible from a measure of the size of the yielded zone. Again following Hill, the expansion of a spherical cavity in an infinite medium is given by

$$a^3 = 3(1-\nu)\ c^3\ (Y/E)$$

in which it is assumed the original size of the cavity is very small relative to the final radius a. This can also be written in the form:

$$V_c = 3(1-\nu)\ V_z\ (Y/E)$$

in which V_c is the volume of the cavity and V_z is the volume of the yielded zone. Referring to Table 3.6.1A for .177" diameter indenters, it can be seen that $V_z/V_c \simeq 30$ for PC and 9-15 for PMMA. This corresponds to a value for (Y/E) for PC of .017 and .034 to .057 for PMMA. This measure leads to somewhat greater values for the yield stress.

The values for PC can be compared with the yield stress for uniaxial compression in which the value 13 ksi (Y/E = .037) has been reported. Hence, yielding under conditions of spherical indentation appears to be occurring at a lower stress level instead of at a higher level as might be expected.

These results are preliminary. The various measures of yield stress are not completely self consistent. On the other hand, the measurements, especially of the yield zone, are quite approximate at best and did not represent the results of a systematic investigation, so that better agreement might be expected under more controlled conditions. Finally, of course, the boundary conditions in our experiments depart considerably from those assumed by Hill.

5. ACKNOWLEDGMENT

This work represents very substantial contributions by Mr. R. L. Mehan, especially as regards the measurements on the electro-hydraulic test machine and the development of the representation of the data in the useful forms given in Section 4.1.1. In addition, the experimental and computational assistance by Mr. J. W. Nehrich is acknowledged. The discussions with Drs. D. G. LeGrand and A. F. Yee have been most helpful and are appreciated.

6. REFERENCES

1. W.B. Hillig, "Impact Studies of Polymeric Matrices," General Electric CRD Report SRD-73-091, prepared under Contract N00019-72-C-0218 for Naval Air Systems Command, Dept. of the Navy, March 1973.

2. W.B. Hillig, "Impact Response Characteristics of Polymeric Matrices," General Electric CRD Report SRD-74-087, prepared under Contract N00019-73-C-0282 for Naval Air Systems Command, Dept. of the Navy, September 1974.

3. J.R. Asay and A.H. Guenther, J. Appl. Polymer Sci. 11, 1087 (1967).

4. J.M. Crissman, J.A. Sauer, and A.E. Woodward, J. Polymer Sci. Pt. A 2, 5075 (1964).

5. O.E. Meyer, Z. Ver. deutch. Ing. 52, 645 (1908).

6. S.C. Hunter, J. Mech. and Phys. Solids 8, 219 (1960).

7. R. Hill, The Mathematical Theory of Plasticity, Oxford Univ. Press, London, 1950, p. 97 ff.

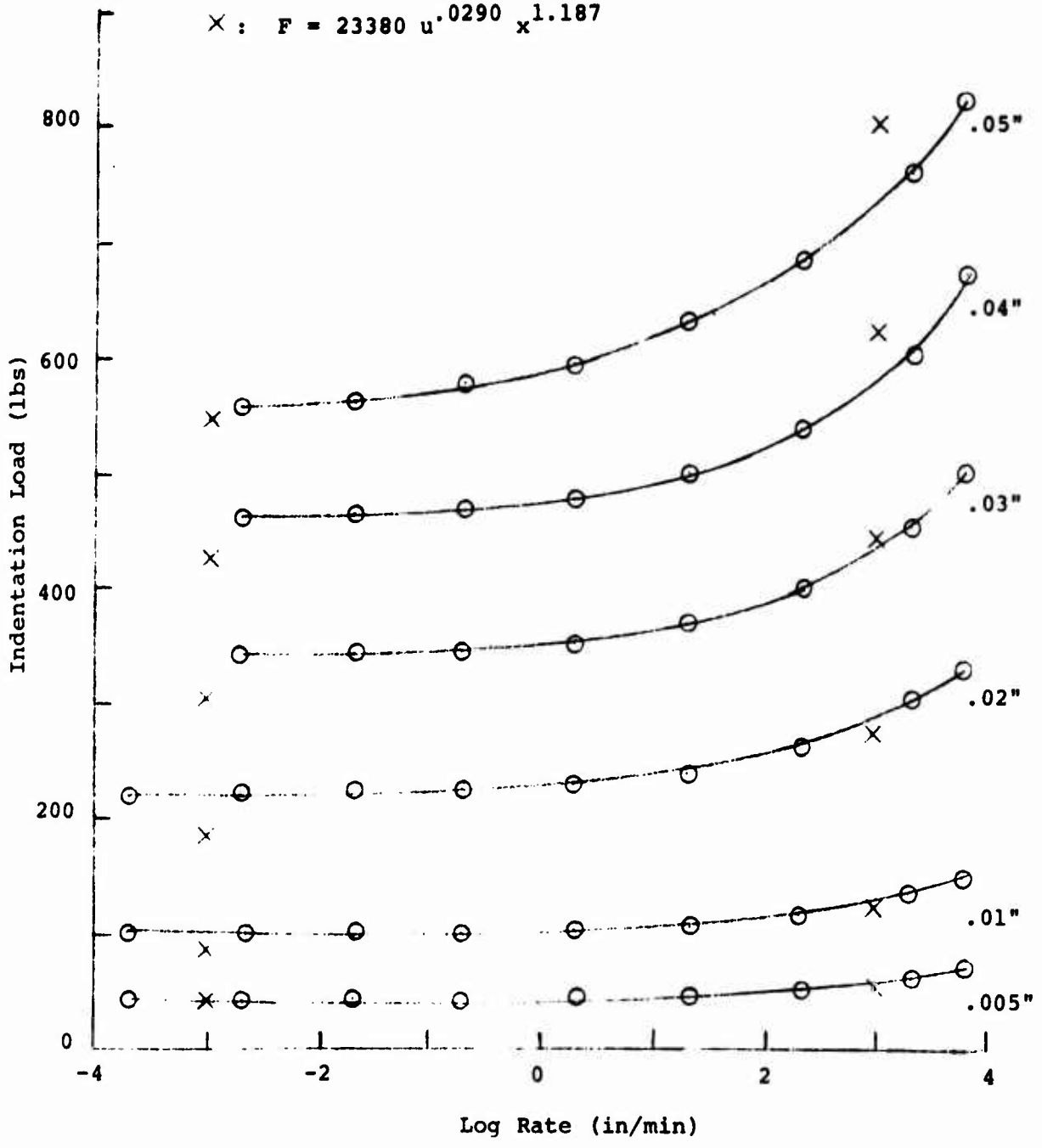

Fig. 3.1.2A Average load-rate curves as a function of penetration for PC.

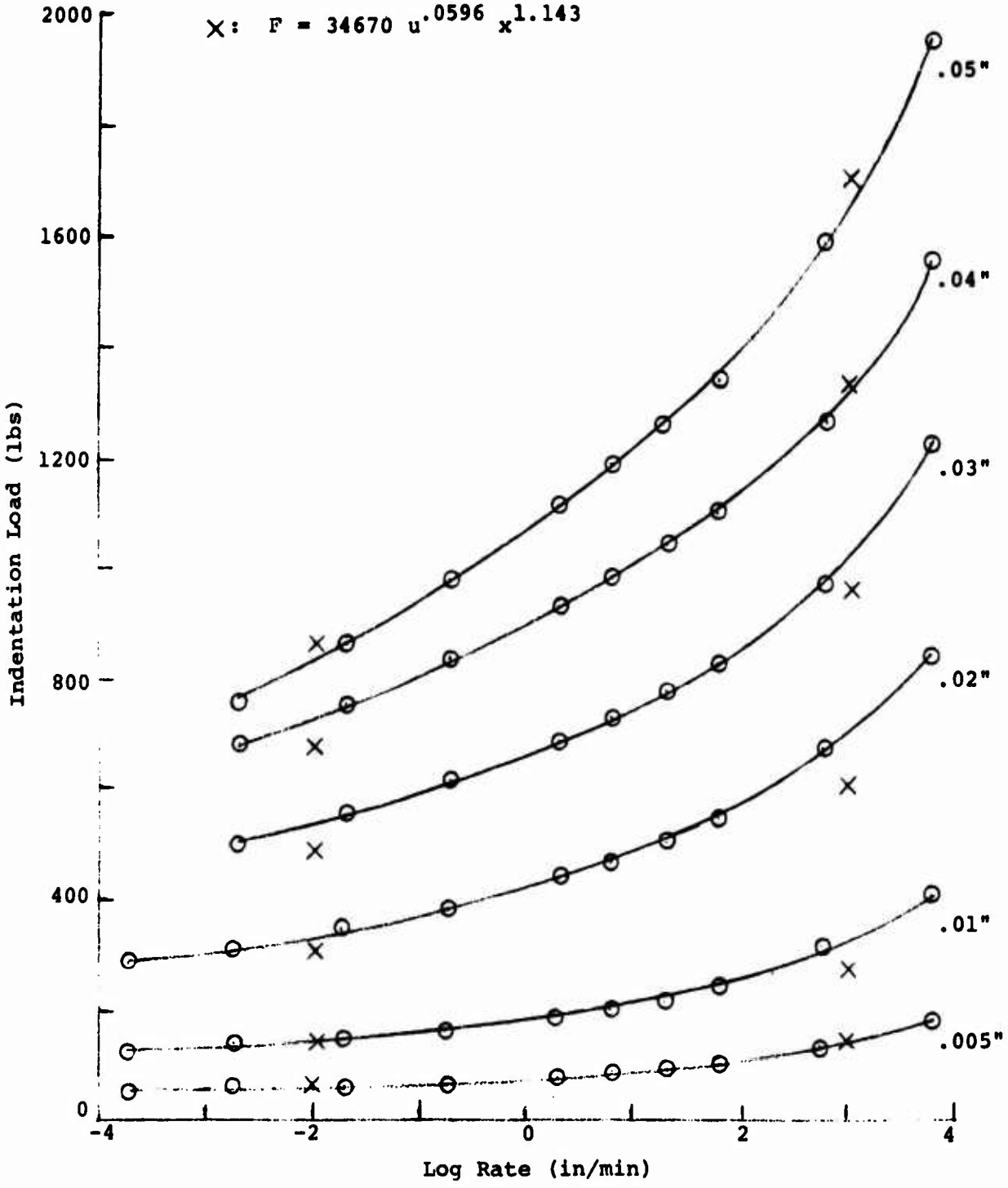

Fig. 3.1.2B Average load-rate curves as a function of penetration for PMMA.

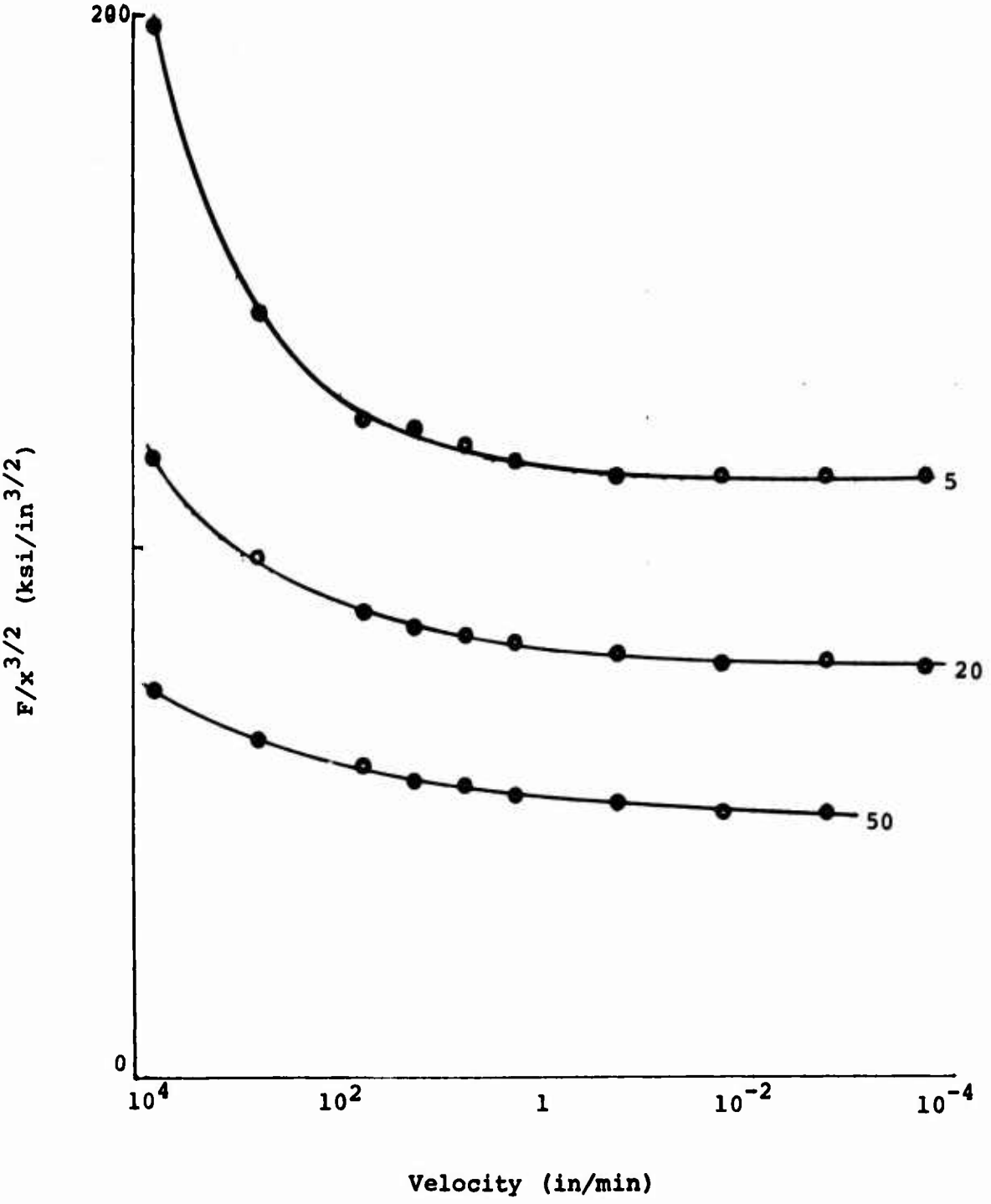

Fig. 3.1.2C $F/x^{3/2}$ for PC as a function of velocity at indicated depth in mils.

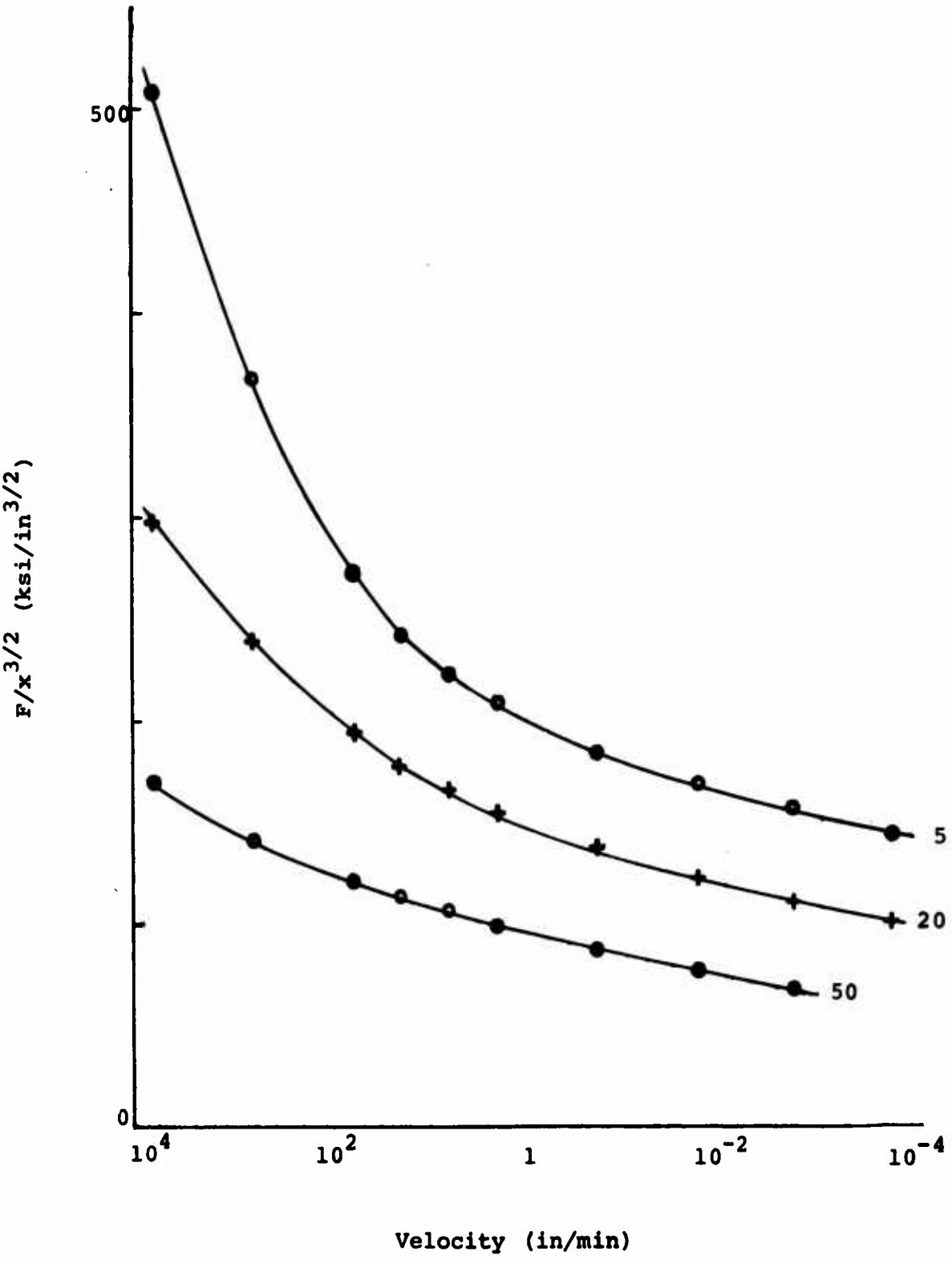

Fig. 3.1.2D $F/x^{3/2}$ for PMMA as a function of velocity at indicated depth in mils.

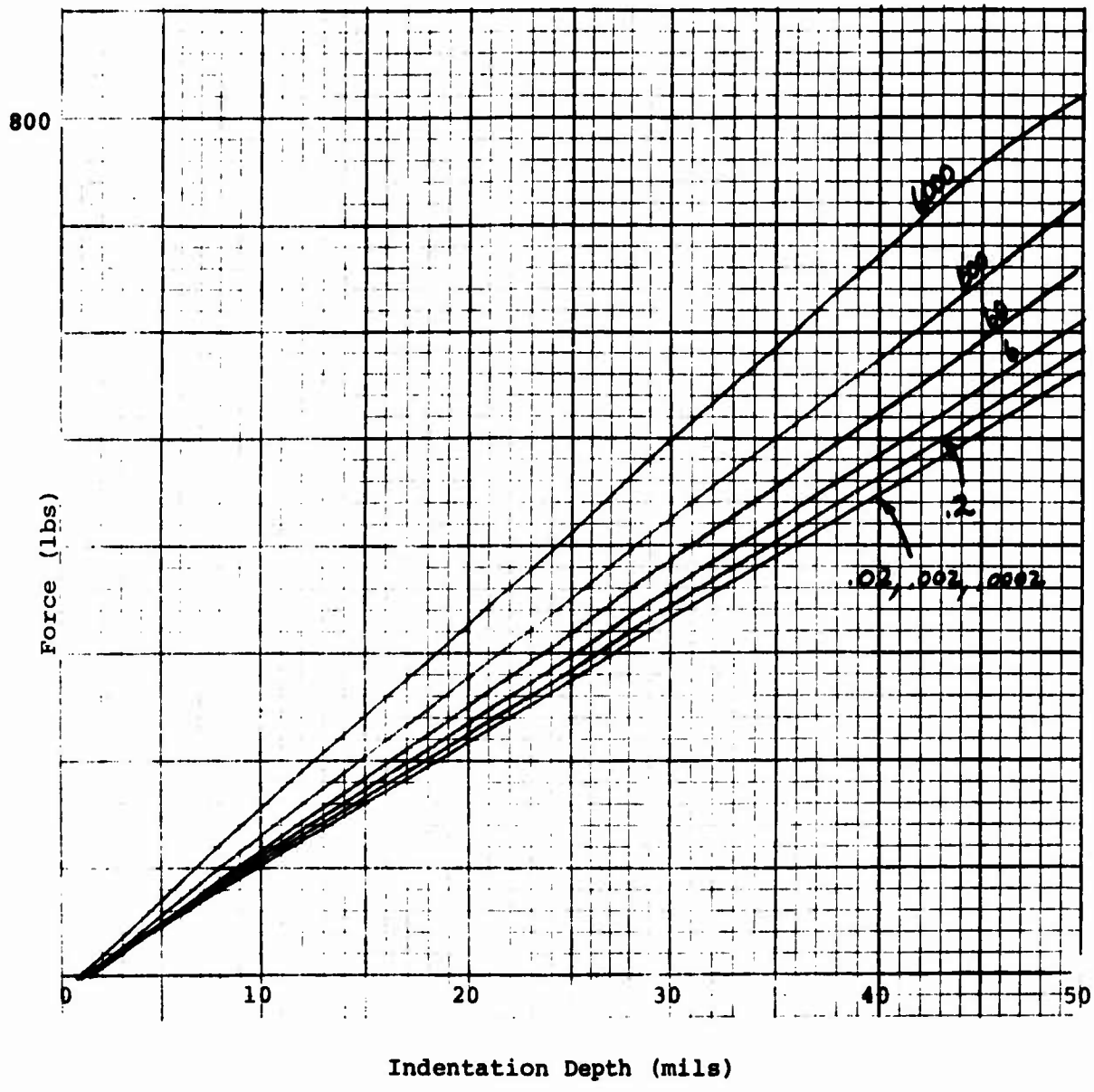

Fig. 3.1.2E The dependence of force vs indentation depth for PC at various velocities (given in in/min).

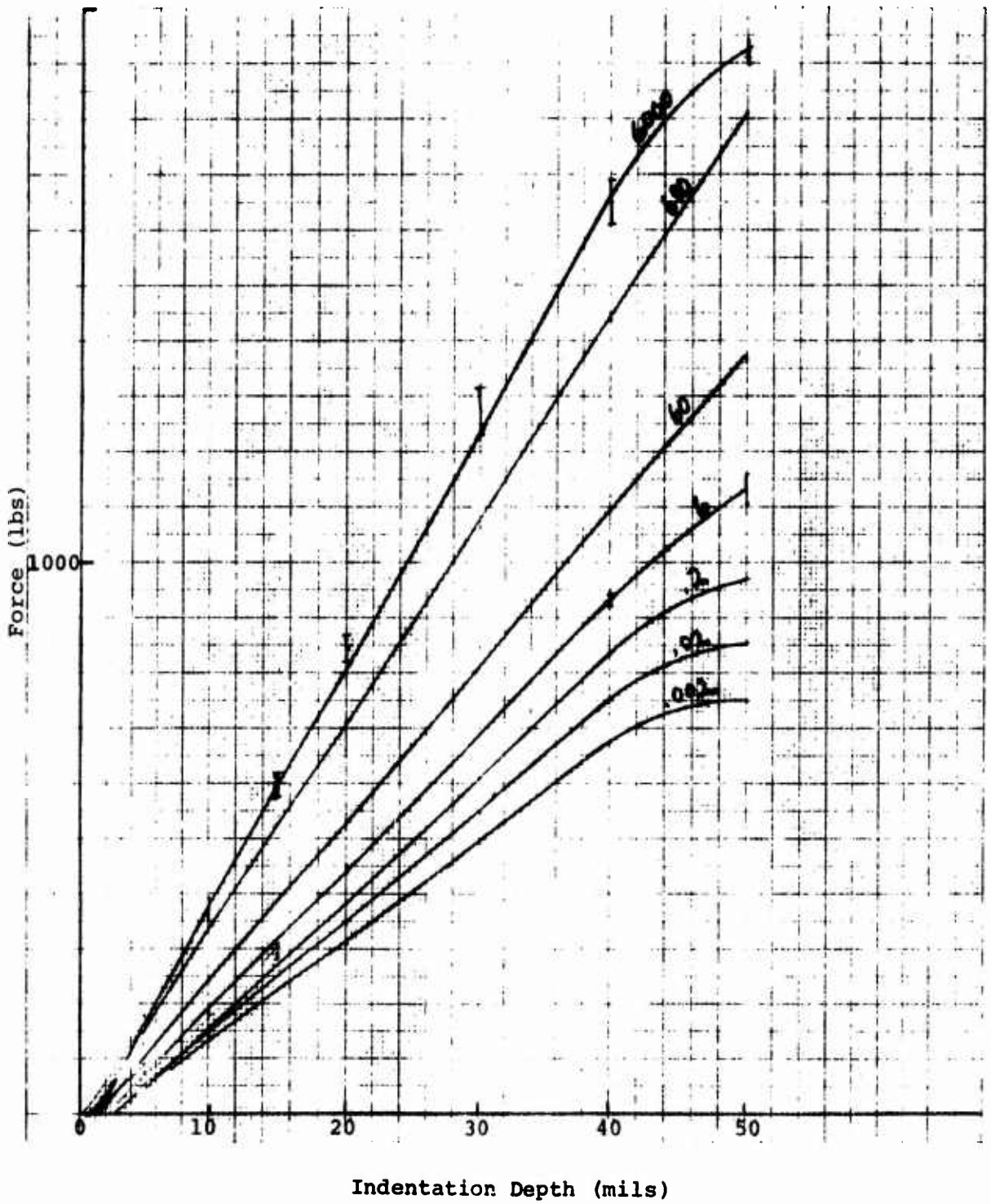

Fig. 3.1.2F The dependence of force vs indentation depth for PMMA at various velocities (given in in/min).

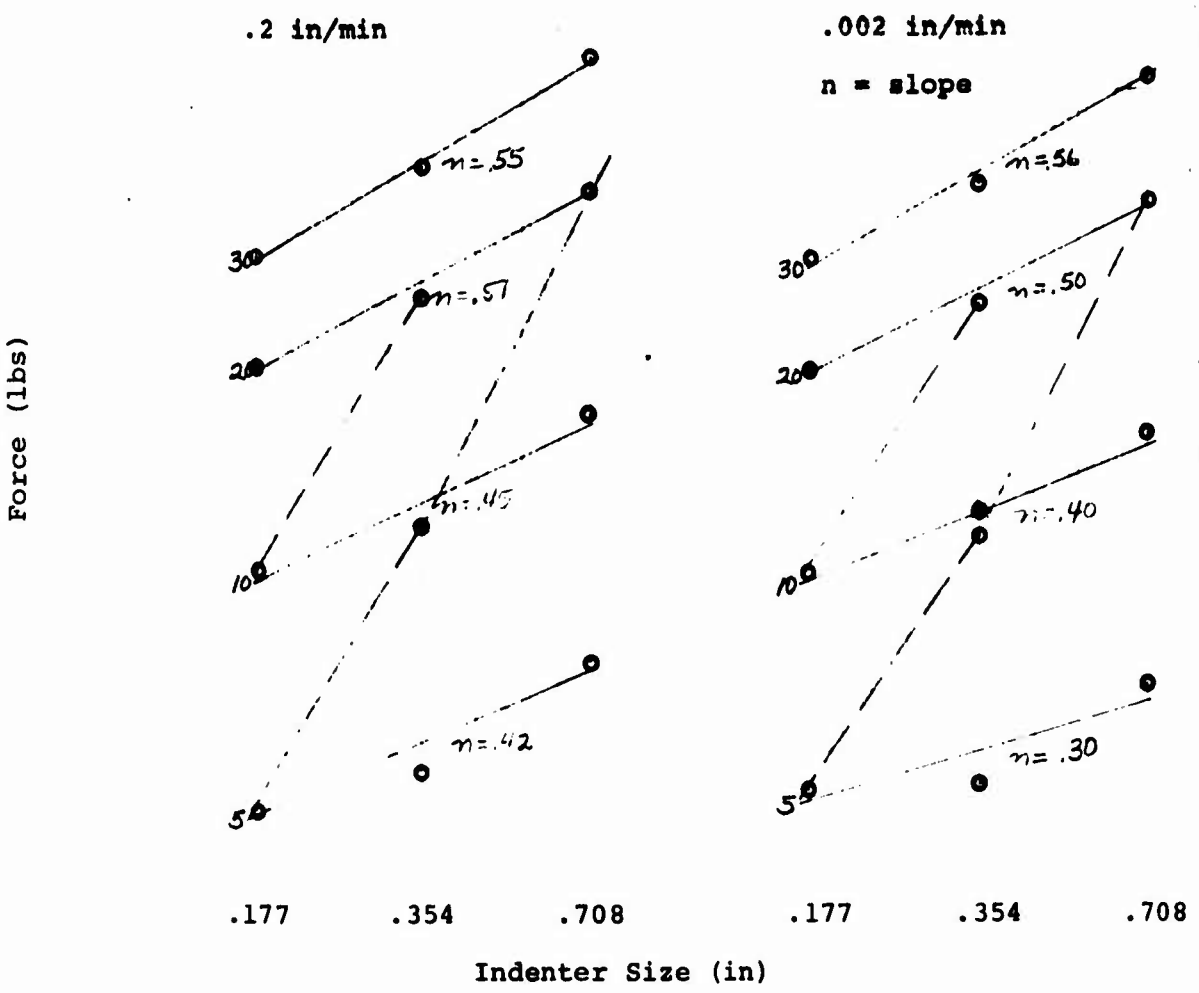

Fig. 3.2.1A Dependence on indenter force on indenter size for PC at indicated depth in mils.

Reproduced from best available copy.

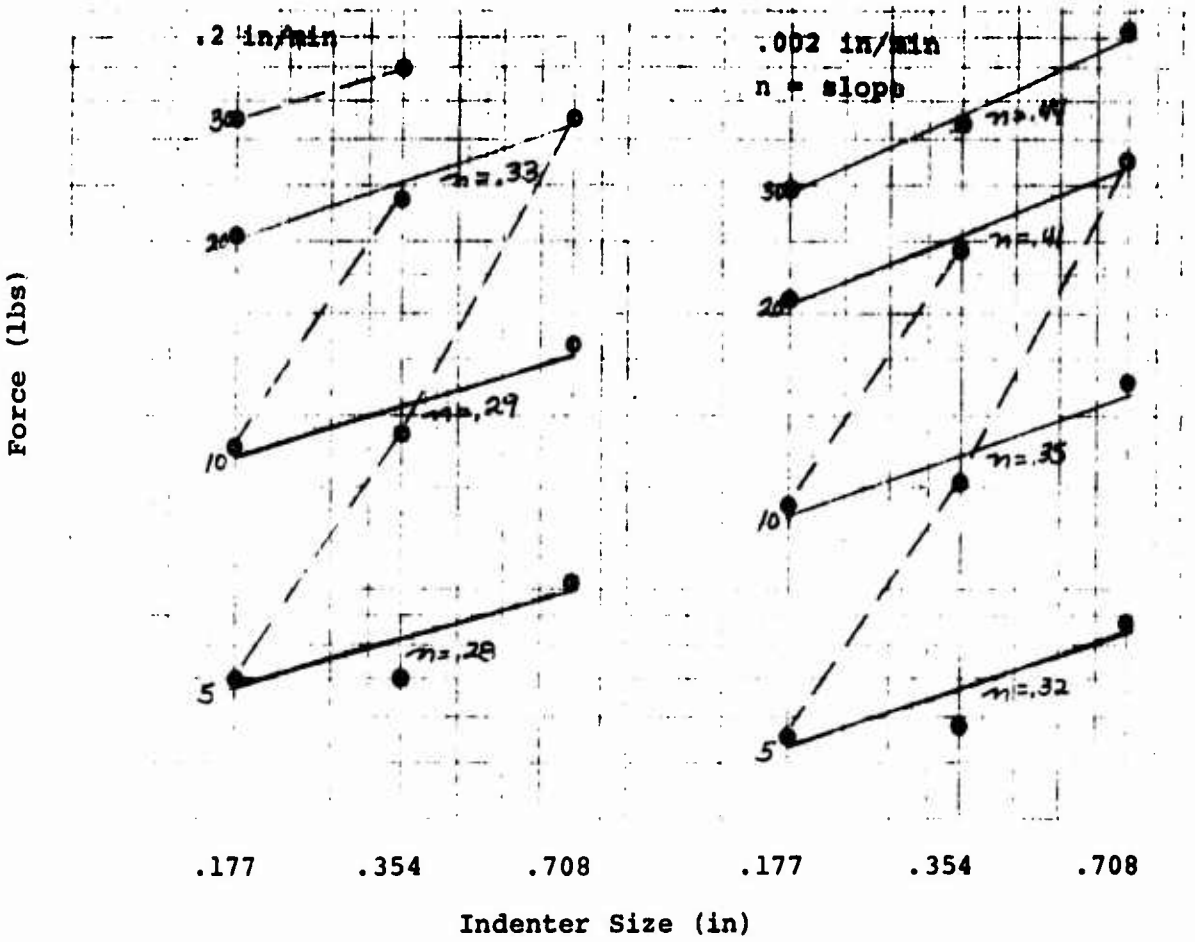

Fig. 3.2.1B Dependence on indenter force on indenter size for PMMA at indicated depth in mils.

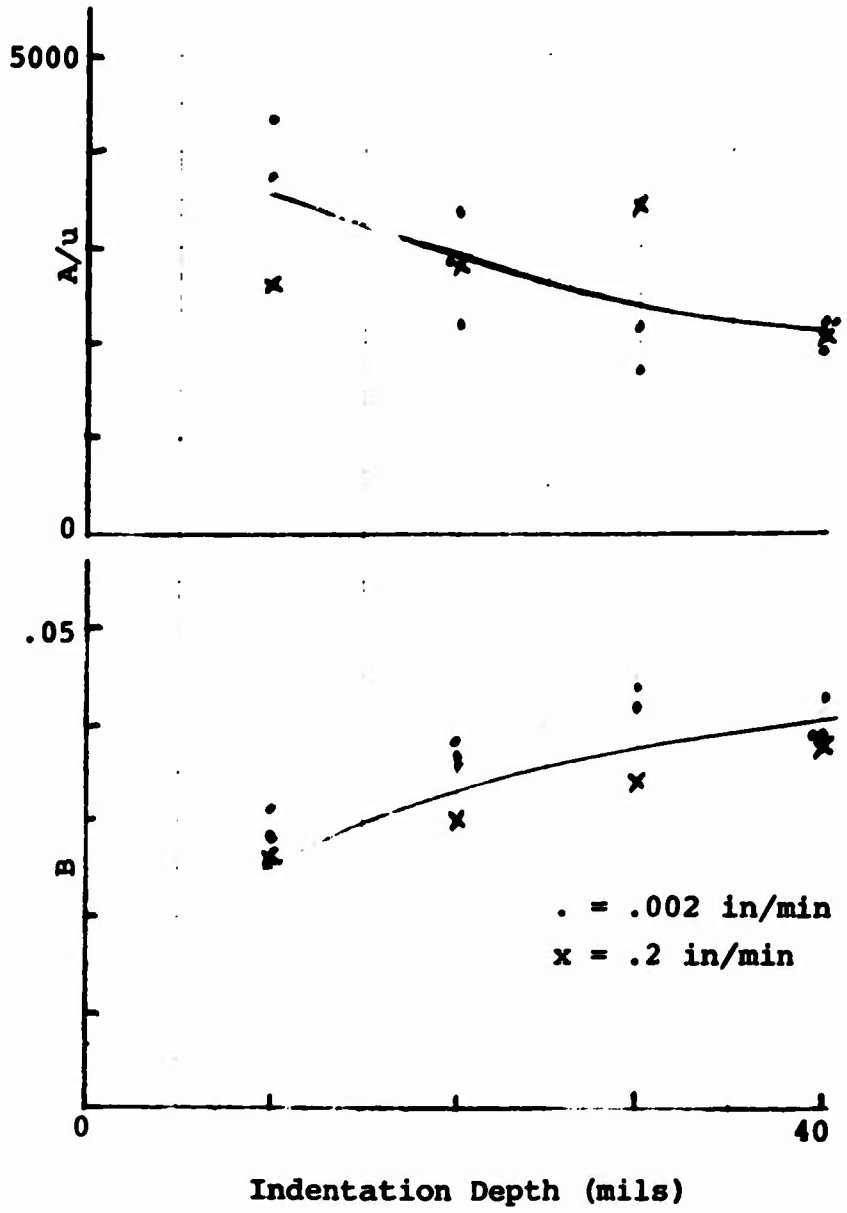

Fig. 3.3.2A Relaxation parameters for PC following indentation to the depth indicated at a velocity of .002 and .2 in/min using a standard ball indenter.

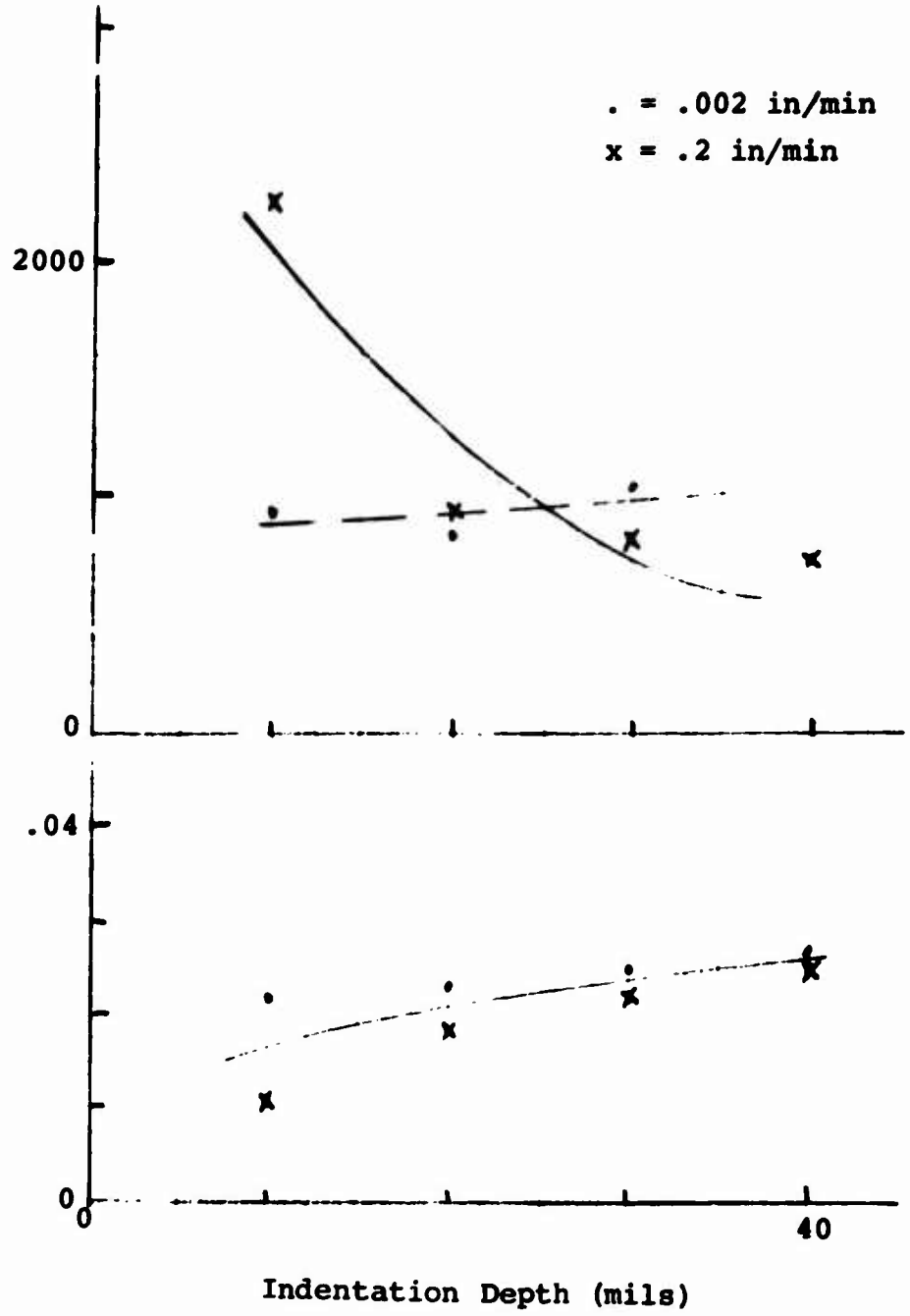

Fig. 3.3.2B Relaxation parameters for PC following indentation to the depth indicated at a velocity of .002 and .2 in/min using a large ball indenter.

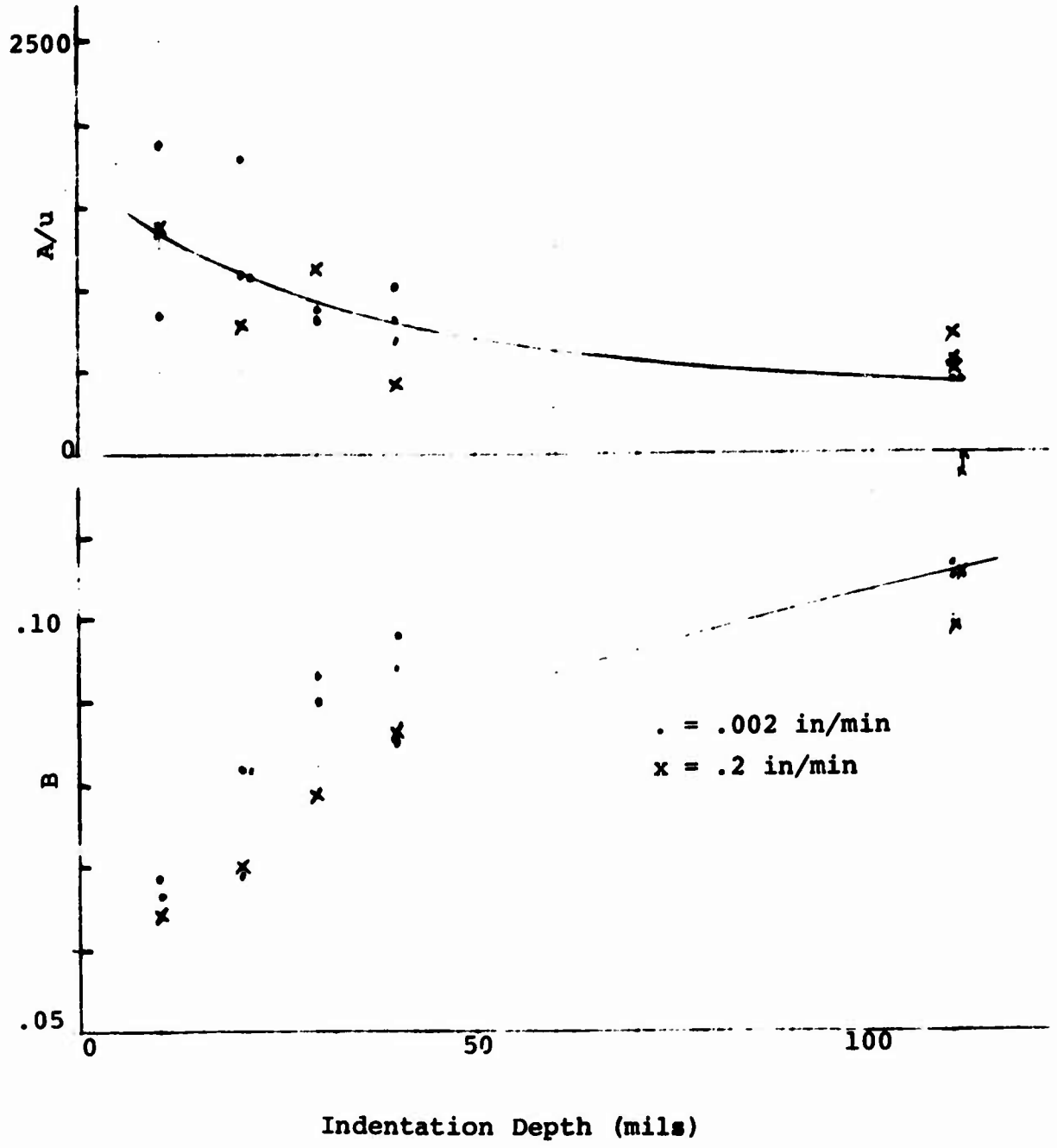

Fig. 3.3.2C Relaxation parameters for PMMA following indentation to the depth indicated at a velocity of .002 and .2 in/min using a standard ball indenter.

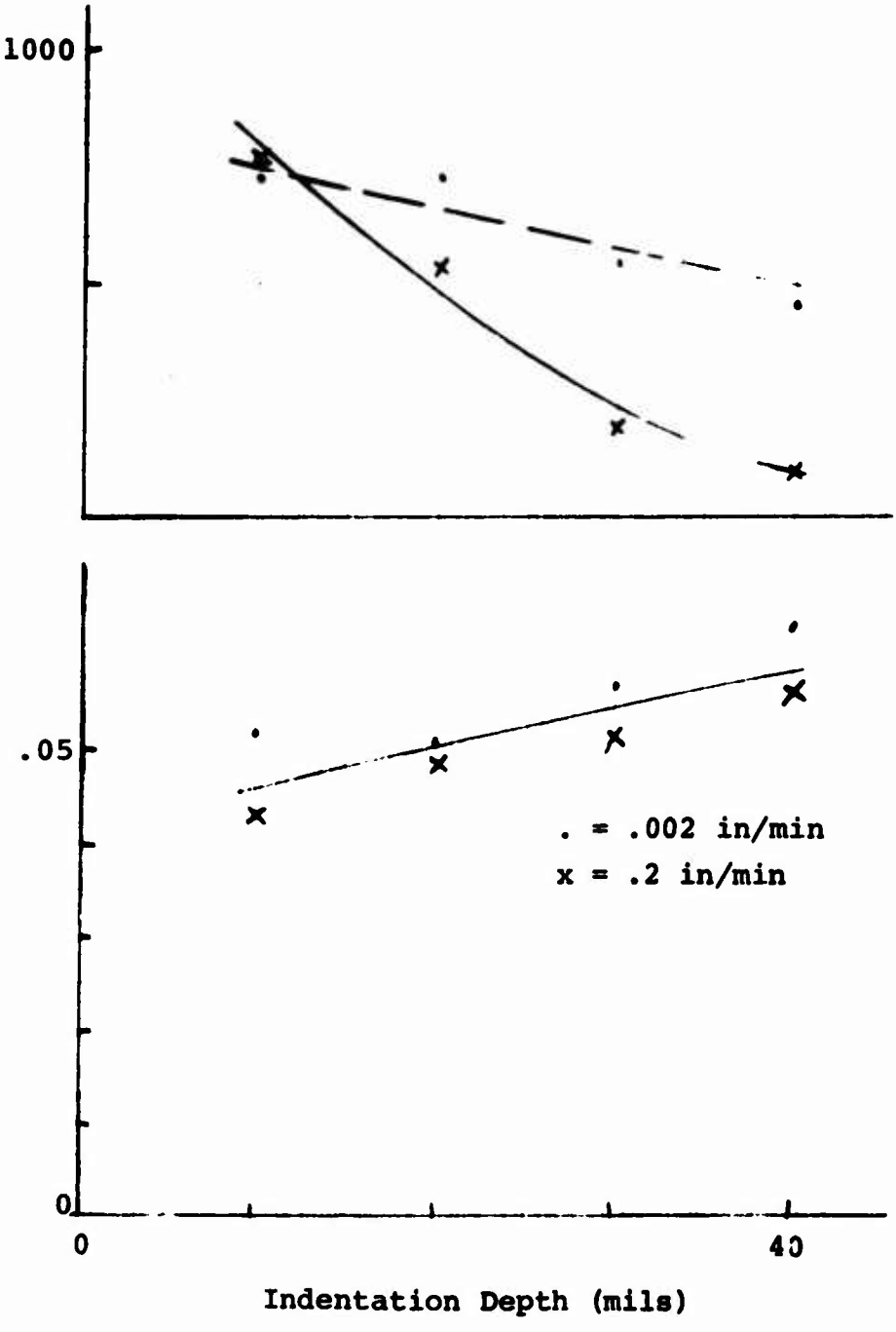

Fig. 3.3.2D Relaxation parameters for PMMA following indentation to the depth indicated at a velocity of .002 and .2 in/min using a large ball indenter.

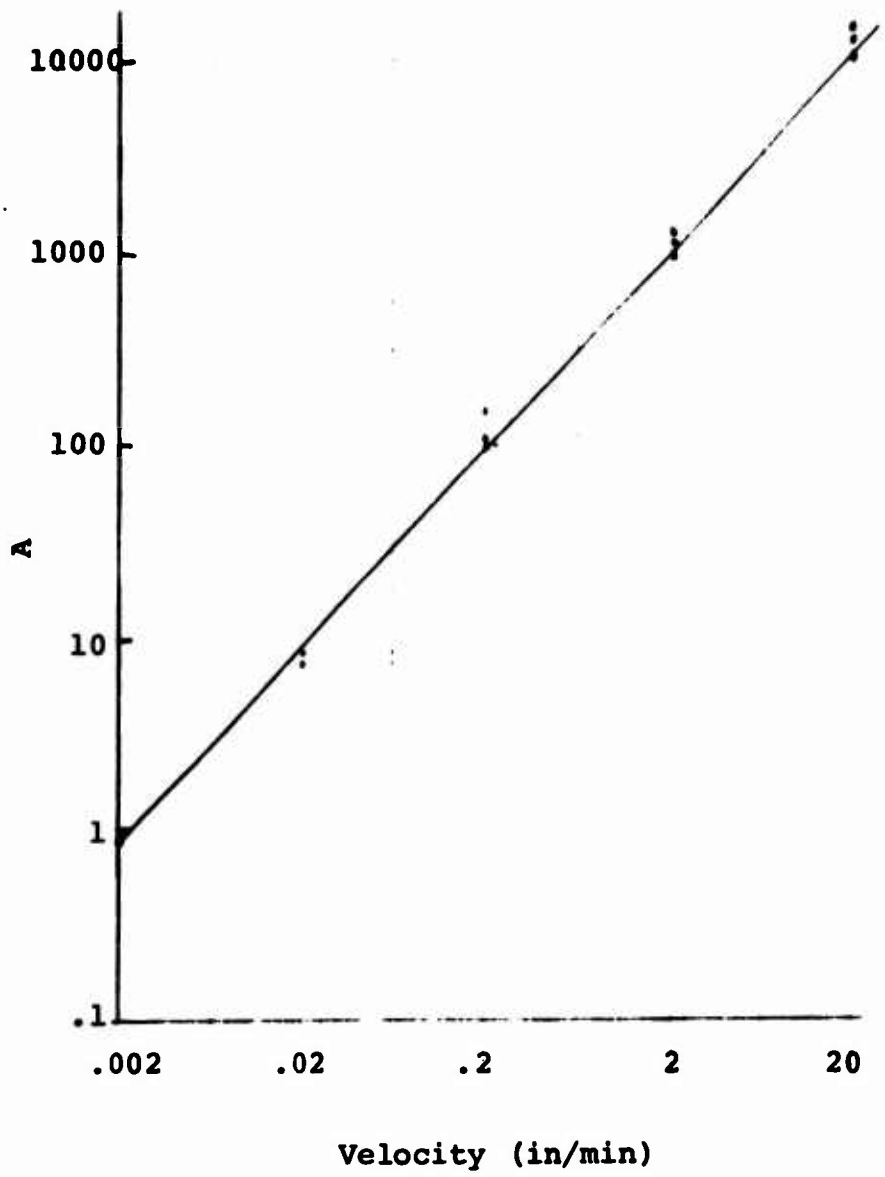

Fig. 3.3.2E Dependence of relaxation parameter A on velocity for case of PMMA at large penetration depths using standard ball.

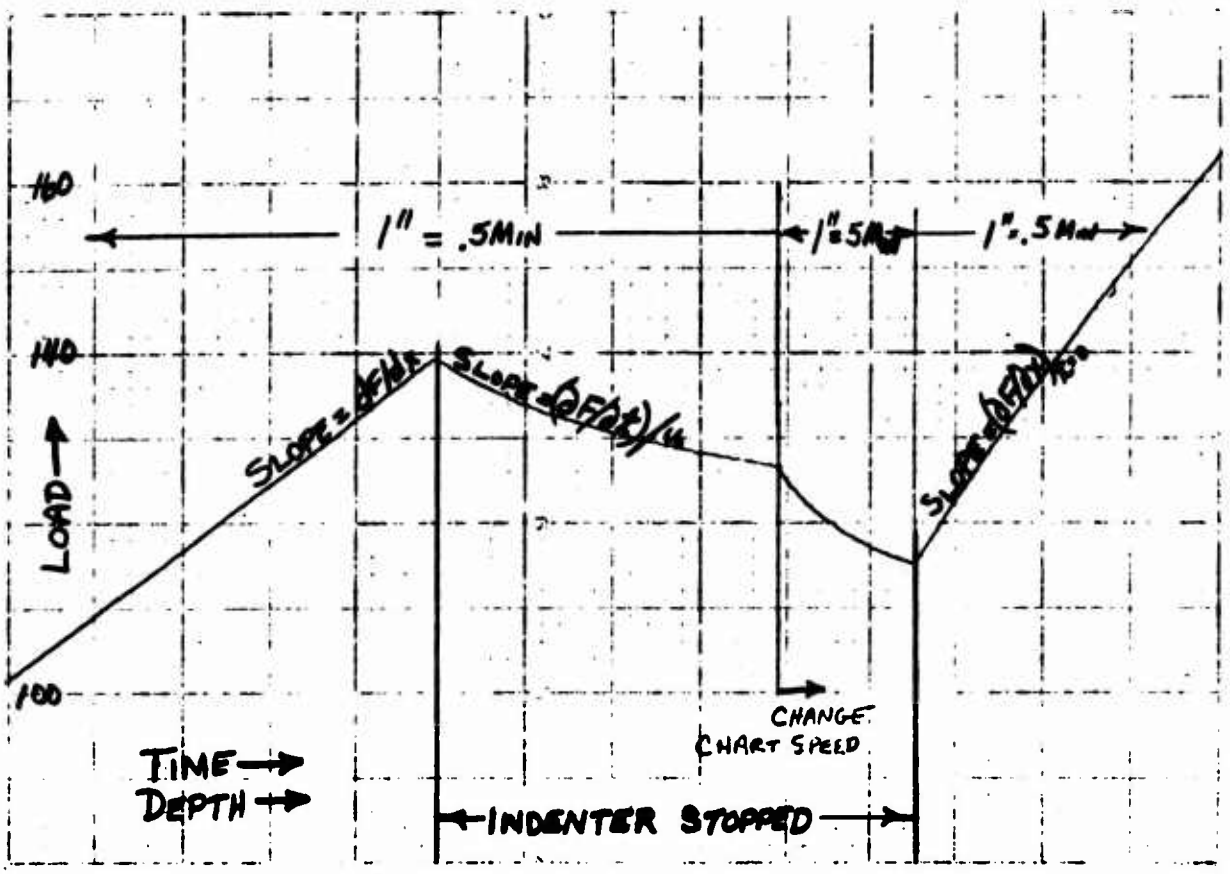

Fig. 3.3.2F Observed behavior of indentation load of PMMA, indented to 10 mils at .002 in/min, indenter stopped 5 min and then started again.

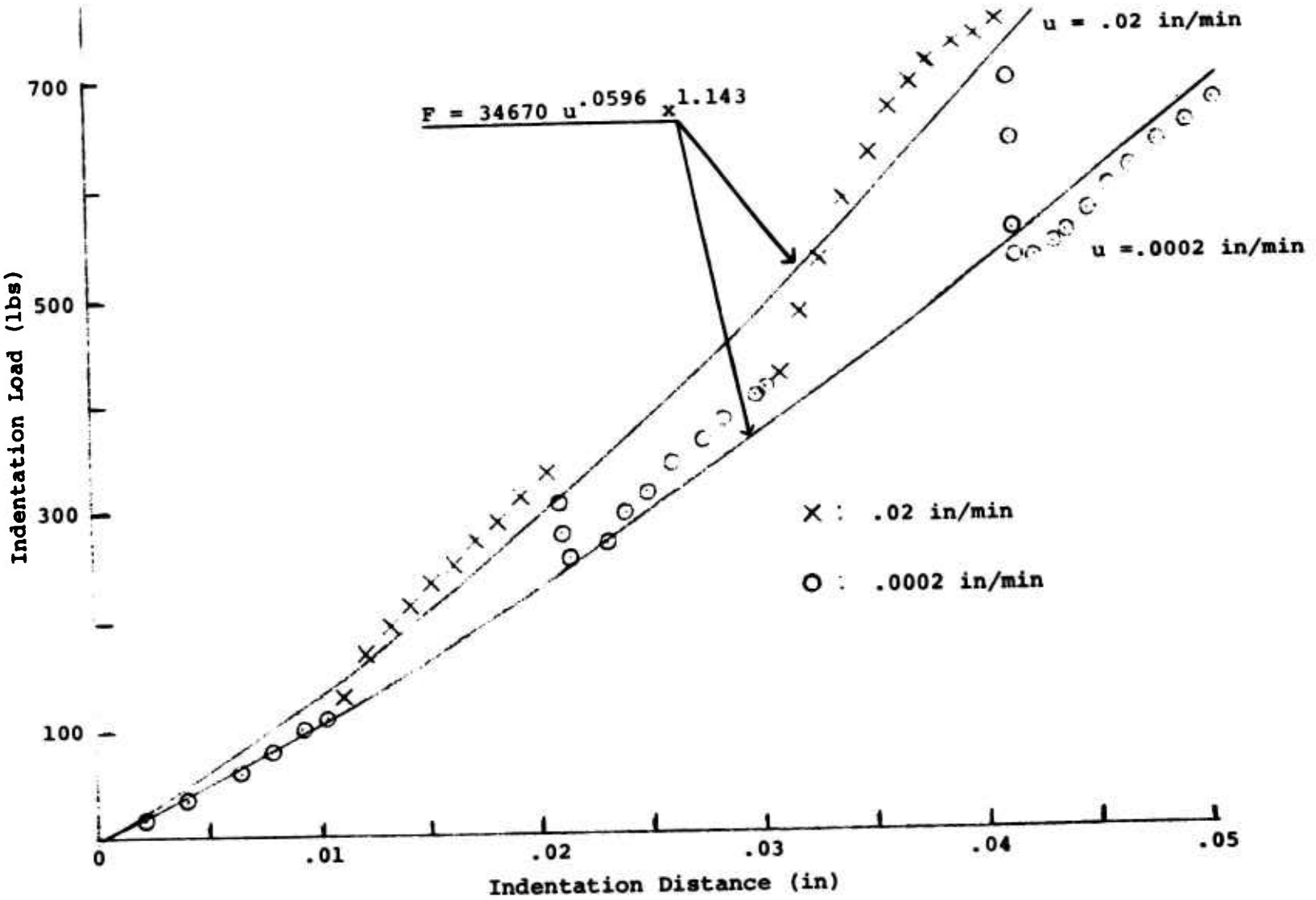

Fig. 3.4.1A Observed and predicted load-deflection curve for PMMA during instantaneous rate change tests.

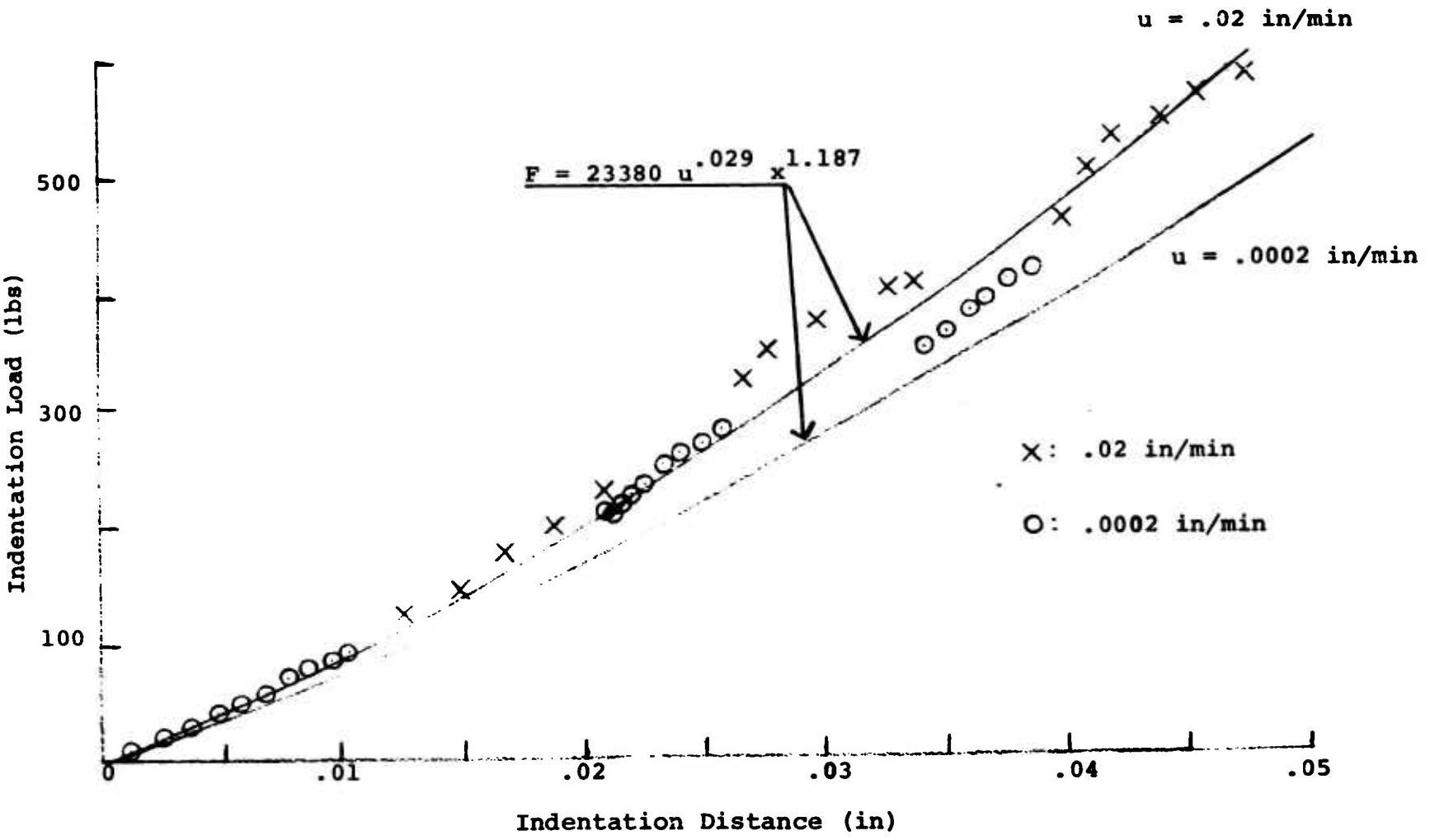

Fig. 3.4.1B Observed and predicted load-deflection curve for PC during instantaneous rate change tests.

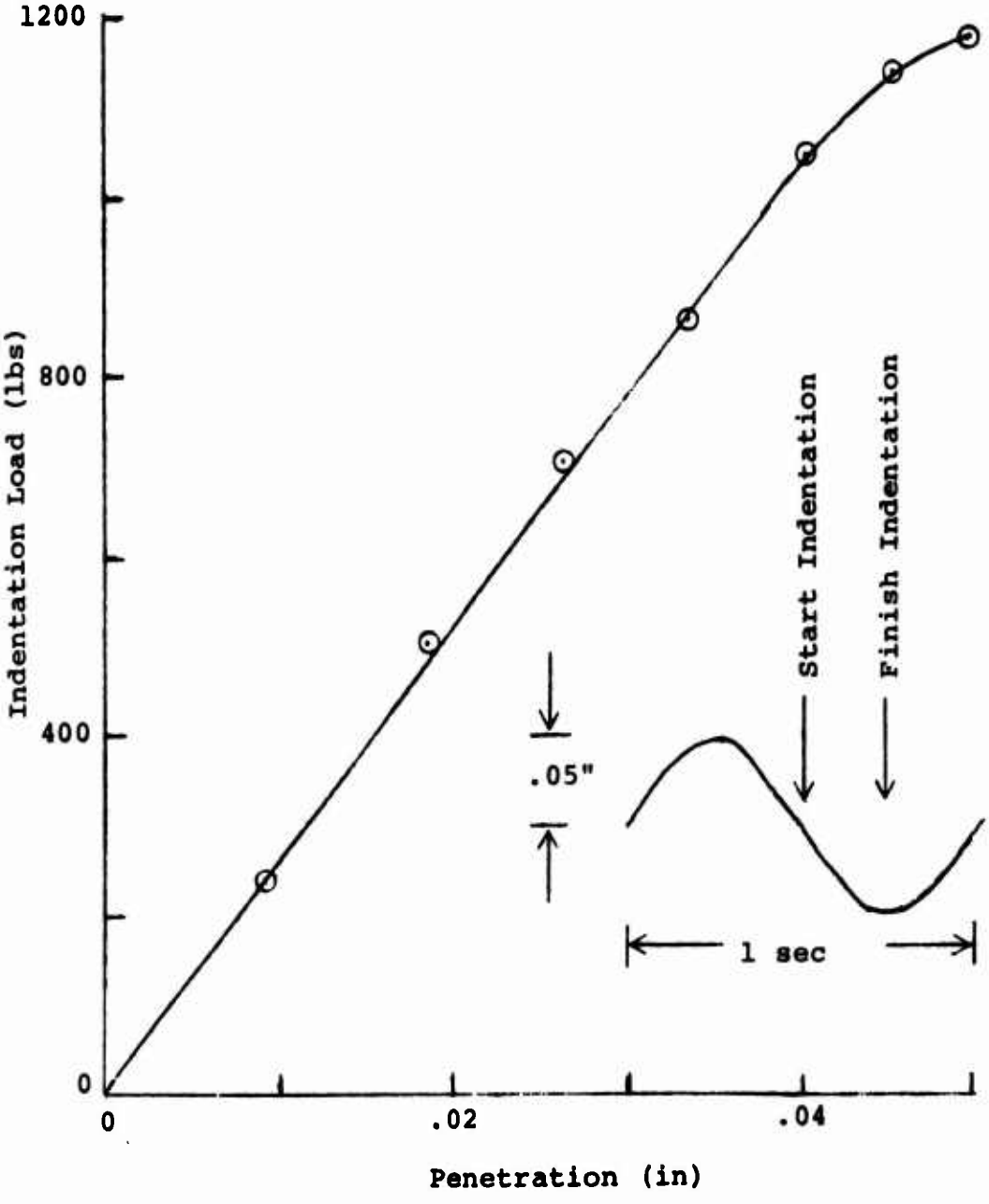

Fig. 3.4.2A Load-penetration curve for PC under sinusoidal loading at 1 cycle/sec.

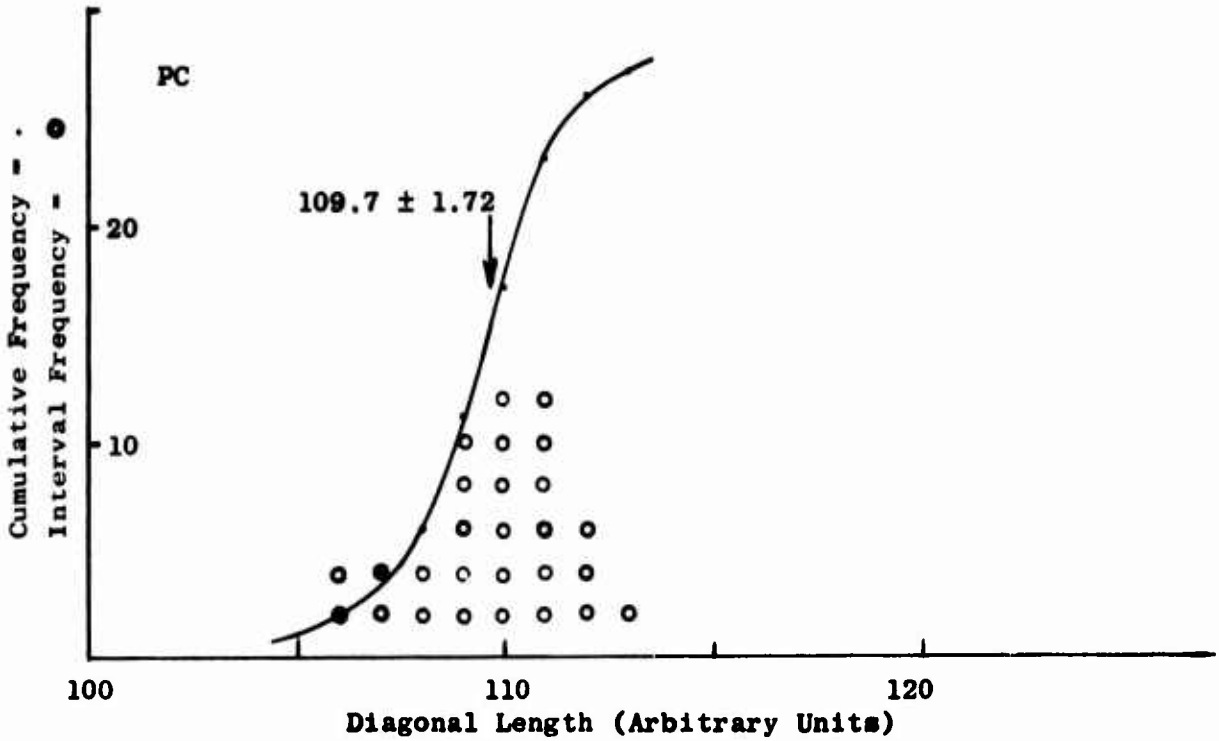

Fig. 3.5A Observed distribution of size of micro-hardness impression on PC material used in the present studies.

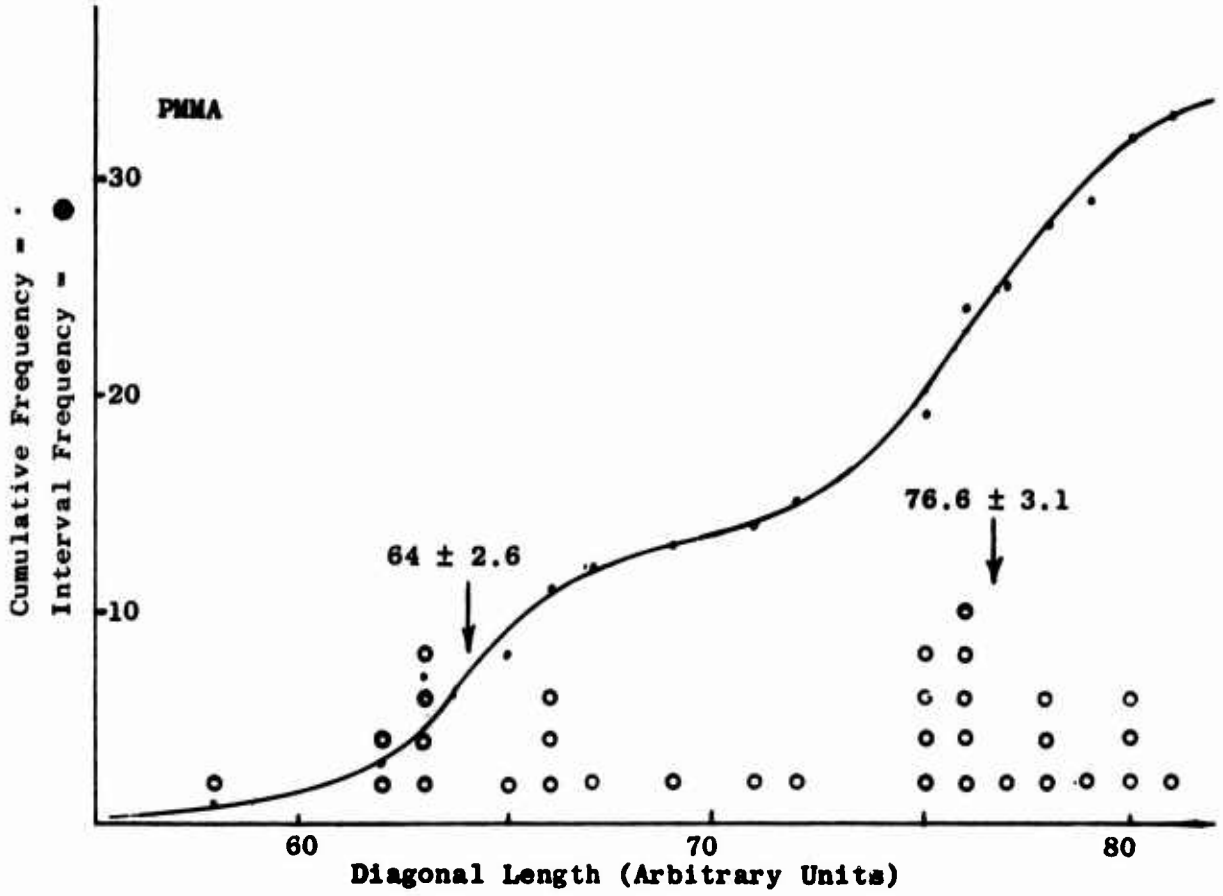

Fig. 3.5B Observed distribution of size of micro-hardness impression on PMMA material used in the present studies.

Fig. 3.6.1A Disturbed zone in PC made by impressing a 9 mm (.354") O.D. ball at .002 in/min.

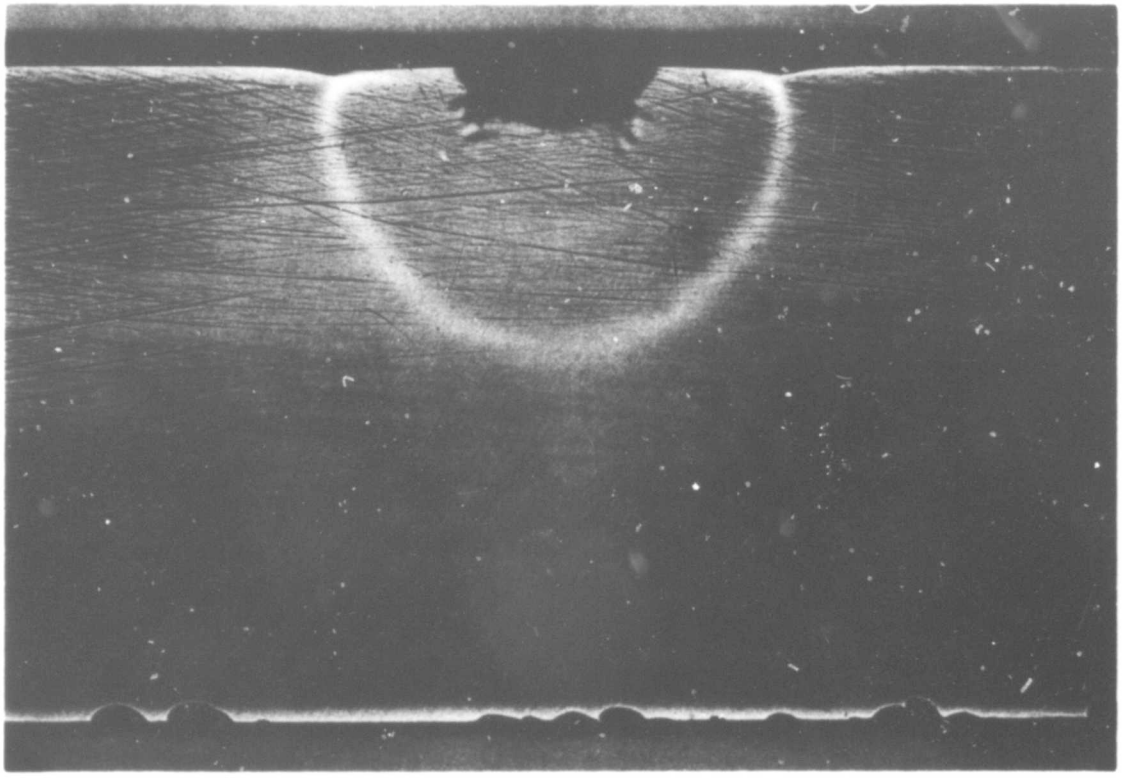

Fig. 3.6.1B Disturbed zone in PMMA made by impressing a 4.5 mm (.177") O.D. ball at 6 in/min.

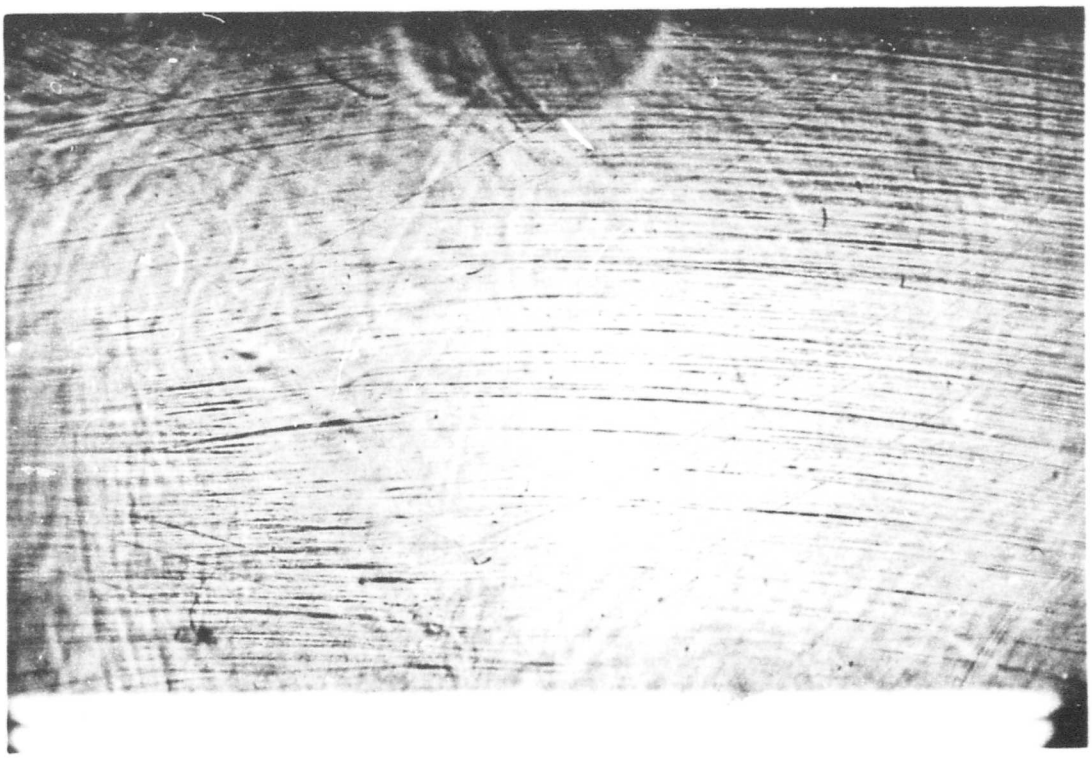

Fig. 3.6.1C Disturbed zone in epoxy made by impressing a 4.5 mm (.177") O.D. ball at .002 in/min.

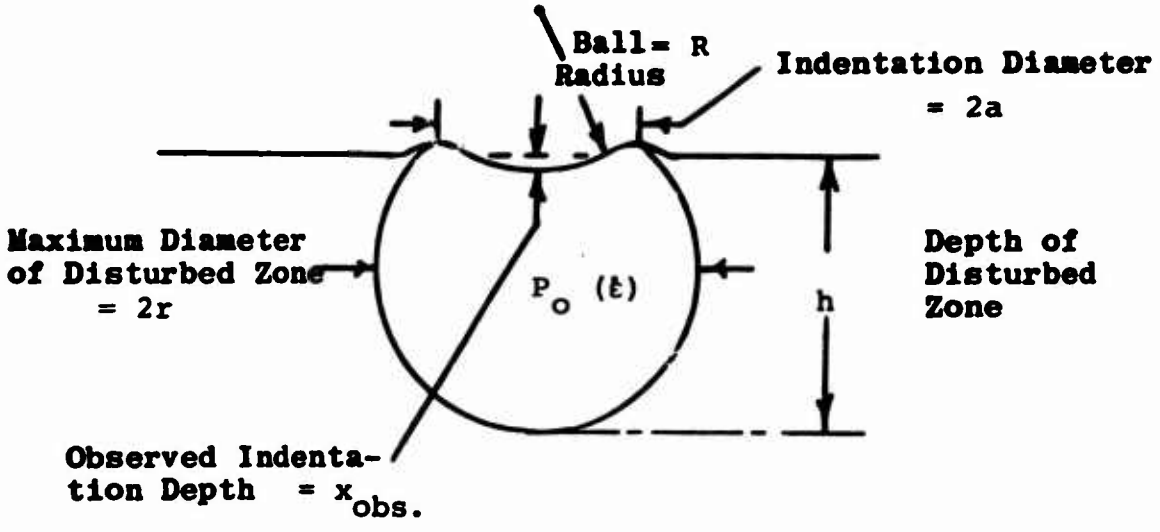

Fig. 3.6.1D Schematic representation of disturbed zone showing the various geometric measures.

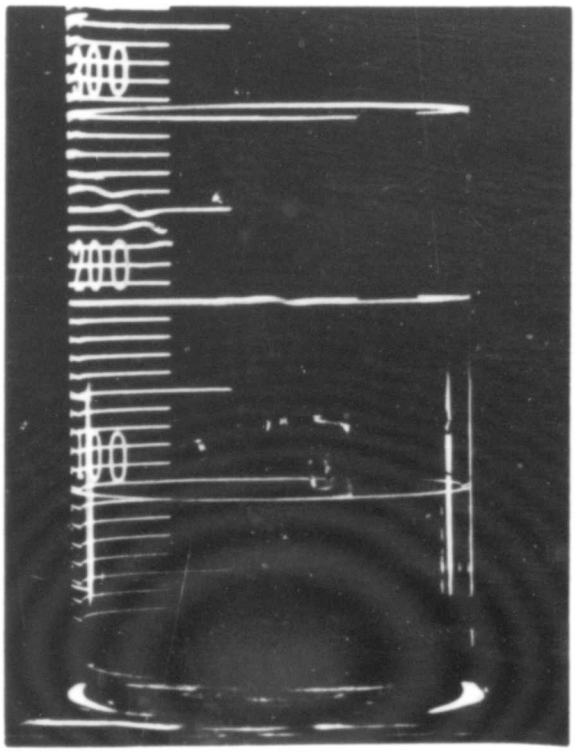

Fig. 3.6.1E Specimens of PC suspended in density gradient column. Three upper pieces are ordinary material; three lower pieces are indented material. 1X.

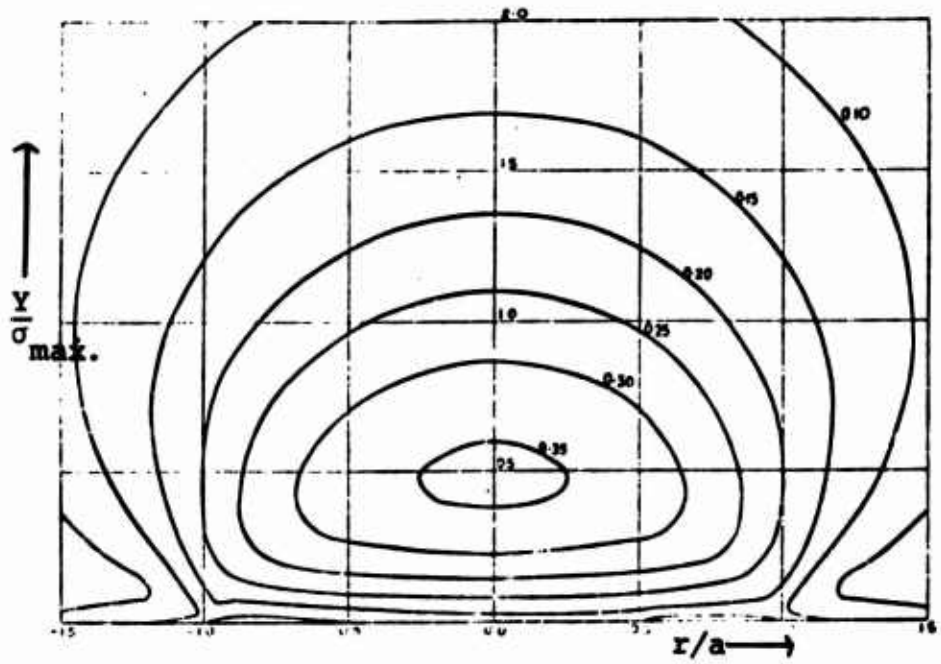

Fig. 3.6.2A Lines of constant ratio of yield stress to maximum compressive stress in the plane normal to the plane of contact.

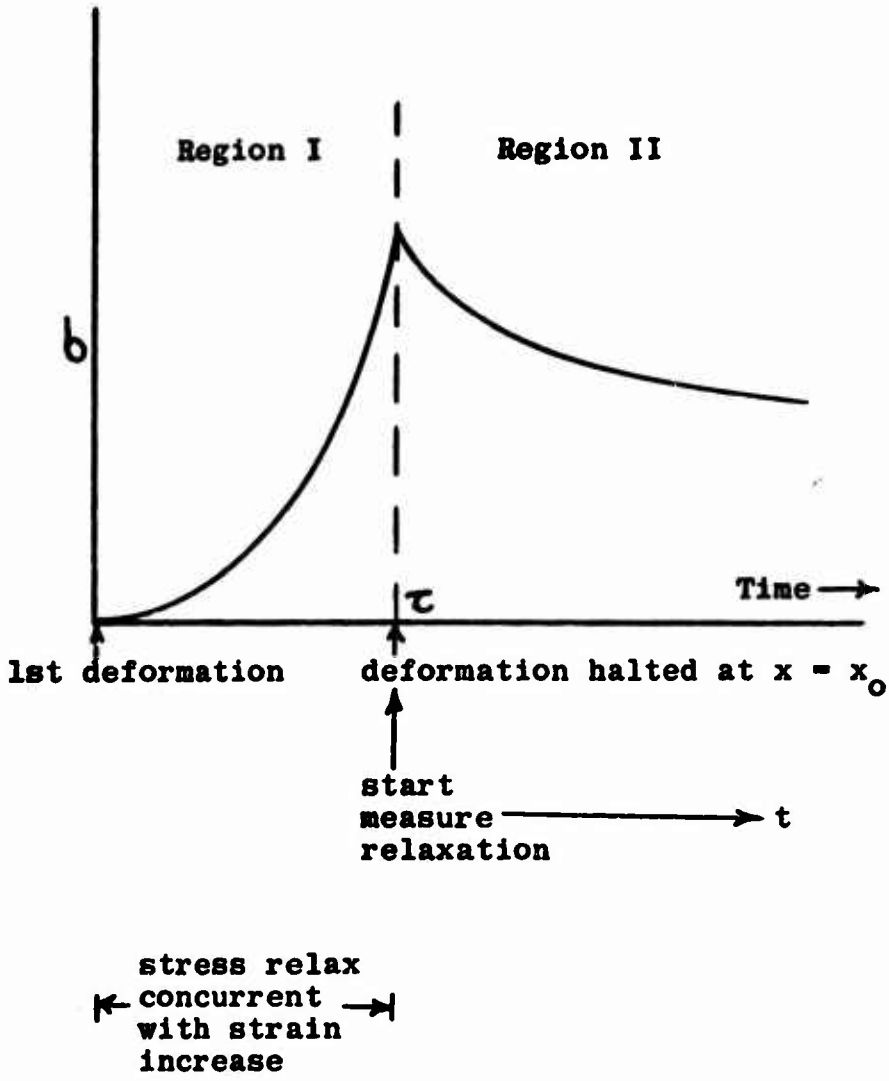

Fig. 4.2.1A Schematic representation of relaxation observations showing how the various measures and regions are related.